Chemical Physics 157 (1991) 1–24
North-Holland

Theory and simulation of optically induced line shifts in NMR

M.W. Evans [1]
Institute of Physical Chemistry, University of Zurich, Winterthurerstrasse 190, CH 8057 Zurich, Switzerland

Received 28 January 1991; in final form 1 July 1991

A theory and field applied computer simulation (FMD) is developed of magnetisation by a circularly polarised laser directed into the sample tube of a contemporary NMR spectrometer, a technique called "optical NMR". The mechanism considered in this paper involves a nonvanishing term in the energy made up of the product $\Delta H_1 = -i({}^{m}\beta''^{ee}_{ijk})_{mn} \Pi^{A}_{jk} B^{(0)}_i$ of the conjugate product Π^{A}_{jk} of the laser, $B^{(0)}_i$, the magnetic flux density of the permanent magnet, and the imaginary part of a rank three mediating molecular property tensor, $({}^{m}\beta''^{ee}_{ijk})_{mn}$, a transition magnetic/electric/electric hyperpolarisability called the "beta tensor". The beta tensor exists both in diamagnetics and paramagnetics, both chiral and achiral in structure, and is closely related to the mediating tensor of the Faraday effect. The effect of the energy ΔH_1 is to split a conventional NMR spectrum into a much richer pattern, governed by the beta tensor selection rules $\Delta J = 0, \pm 1, \pm 2, \Delta M = 0, \pm 1, \pm 2$, and by Landé coupling with the conventional (nuclear spin) NMR Hamiltonian. The diagrammatic perturbation calculus and properties of beta close to optical resonance are examined, the point group symmetries and selection rules of beta are tabulated for all molecular point groups, the FMD simulation is initiated in water of the molecular dynamics and transient ensemble responses mediated by beta, and generalised Langevin–Kielich functions are given of the beta mediated orientational response of the molecular ensemble. Suggestions are made for the experimental development of optical NMR spectroscopy.

1. Introduction

The first theoretical indications of magnetisation by circularly polarised lasers were given by Pershan [1] in 1963. These were verified experimentally by van der Ziel and co-workers [2,3] by measuring a magnetisation of the order 0.01 A/m induced by a pulse of giant ruby laser radiation of about 10^{11} W/m^2 peak intensity. The samples included paramagnetic doped glasses at low temperature and room temperature diamagnetic liquids with high Verdet constants [4]. The magnetisation was identified as the inverse Faraday effect (IFE), which has subsequently been developed by Atkins and Miller [5], using quantum field theory, and is described in textbooks by Atkins [6] and Shen [7]. It has been recognised by van der Ziel and co-workers [2,3], by Atkins and Miller [5], by Woźniak and co-workers [8–11] and by Wagnière [12] that the mediating molecular property tensor [13] of the IFE is structurally very similar to its counterpart in the well known Faraday effect [13], which is the rotation of the plane of polarisation of a probe laser by the static flux density, $B^{(0)}_i$ (in T). Remarkably, the original experiments of van der Ziel and co-workers [2,3] appear to have remained the only ones recorded in the literature on the IFE.

Recently, Evans [14–19] has developed the theory of the IFE by making use of the mathematical relation

$$\Pi^{A}_i = \epsilon_{ijk} \Pi^{A}_{jk} \tag{1}$$

between the rank two (Π^{A}_{jk}) and rank one (Π^{A}_{i}) tensor representations of the conjugate product

$$\Pi^{A}_{ij} = \tfrac{1}{2}(E_i E^*_j - E_j E^*_i) \tag{2}$$

of a circularly polarised laser. Here ϵ_{ijk} is the rank three totally antisymmetric unit tensor (the Levi–Civita symbol [13]), and E_i is the electric field strength in V/m of the laser plane wave. The symbol E^*_i denotes the complex conjugate of E_i. The conjugate product in its rank two, polar tensor, represen-

[1] Permanent address: 433 Theory Center, Cornell University, Ithaca, NY 14853, USA.

tation is therefore the antisymmetric part of the complete tensor product $E_i E_j^*$. It is related [13] to the rank one, axial vector Π_i^A through the purely mathematical relation (1). (This kind of relation [13] is very well known in, for example, the representation of a vortex in hydrodynamics.) In its vector form, the laser conjugate product is [12,14–19]

$$\Pi^A = E_L \times E_L^* = -E_R \times E_R^* = 2iE_0^2 k \tag{3}$$

where k is a unit vector in the laser propagation axis Z of the laboratory frame (X, Y, Z), and E_0 is the scalar amplitude of the electric field strength of the laser. Note that the vector representation (3) is purely imaginary and changes sign when switching the laser from right (R) to left (L) circular polarisation. As a consequence it vanishes when the laser is not circularly polarised, and is maximal when the laser is fully right or left circularly polarised. This is of key importance in the development of the technique called "optical NMR" in this paper. Other key properties of Π^A are that it changes sign at motion reversal (the operator T) [19] and not at parity inversion P. This is discussed carefully in ref. [19]. In consequence it has the same fundamental symmetries as the magnetic flux density B and of the angular momentum J. Since B is the basis of NMR and EPR and J is the basis of much of the quantum mechanical description of spectroscopy [6], the symmetry of Π^A is potentially of much practical interest [14–19].

This symmetry analysis of Π^A has been used recently by Evans [14–19] to predict the existence of several interesting spectroscopic effects, including: the optical Zeeman effect [14], where Π^A plays the role of B in the conventional Zeeman effect [13]; forward–backward birefringence due to Π^A [15], in which Π^A plays the role of B in the magneto-chiral effect [20–24], also derived independently and cotemporaneously by Woźniak and Zawodny [20] and called by them "magneto-spatial dispersion". Potentially the most useful of the Π^A-induced effects is optical NMR [16–18] and optical ESR [19] in which $B^{(0)}$ of the parmanent magnet in conventional NMR or ESR [25] is supplemented (i.e. not replaced) by Π^A of a circularly polarised laser directed into the sample tube. The first optical NMR experiment has been initiated by Warren et al. [26].

The first theory of optical NMR [17–19] relied on the energy

$$\Delta H = -\tfrac{1}{2} i (\alpha''_{jk})_{mn} \Pi^A_{jk} - m_i^{(N)} B_i^{(0)}$$
$$= -\tfrac{1}{2} i (\alpha_i^*)_{mn} \Pi_i^A - m_i^{(N)} B_i^{(0)} , \tag{4}$$

consisting of the usual NMR energy, $-m_i^{(N)} B_i^{(0)}$, where $m_i^{(N)}$ is the nuclear magnetic dipole moment, and $-\tfrac{1}{2} i (\alpha''_i)_{mn} \Pi_i^A$. The quantity $(\alpha''_i)_{mn}$ is a rank one, axial vector representation of the imaginary part of the transition electronic polarisability [13], $(\alpha''_{jk})_{mn}$, a quantity we call the "alpha tensor":

$$(\alpha''_i)_{mn} = \epsilon_{ijk} (\alpha''_{jk})_{mn} . \tag{5}$$

The alpha tensor is nonzero, however, only when there is a net electronic angular momentum, for example in atoms or paramagnetic molecules such as nitric oxide [26], it is a purely imaginary quantity [13], and has the same P and T symmetries as Π_i^A. Its far from optical resonance order of magnitude can be estimated from knowledge of the Verdet constant, the Faraday A and C terms [8] and the magnetic dipole moment to be [27] about 10^{-42} to 10^{-41} $C^2\,m^2\,J^{-1}$ in SI units. In consequence the nuclear magnetic resonance frequency shift and extra spectral structure due to the part $\tfrac{1}{2} i (\alpha''_i)_{mn} \Pi_i^A$ of the energy, eq. (4), can be worked out [18,19] given this order of magnitude for the alpha tensor and the magnetic flux density $B_i^{(0)}$ of the permanent NMR magnet. The result is a shift in the NMR line and a broadening which represents the unresolved spectral structure due to magnetic transitions and Landé coupling between the parts of the energy eq. (4) due to the laser and magnet. This is analogous in concept, but not of course in detail, with the theory [6] of the anomalous Zeeman effect, where there is Landé coupling between orbital and spin angular momentum. In general, the extent of this broadening (or unresolved spectral detail) depends on both $B_i^{(0)}$ and Π_i^A, i.e. on the nature of the resonating nucleus and on the nature of the electronic property $(\alpha''_i)_{mn}$. It is therefore expected to be site selective, i.e. the extent of the broadening will depend on the position of the nucleus and surrounding electrons in the molecule, and to give potentially useful, perhaps unique, information on complex structures in solution, such as folded proteins [28–30]. The shift and broadening will affect the 2-D NMR maps [28–30], changing the contours and overall "geography" in an analytically useful way. The maps will change in general with laser frequency as well as

laser intensity, because the alpha tensor is a spectral quantity, which peaks near optical resonances [13], and which has a well defined semi-classical structure from perturbation calculus of the time dependent Schrödinger equation [31], or from the matrix density formalism [32]. In general terms, therefore, an optical NMR map is one in which the conventional 2-D NMR map is changed topologically by an applied circularly polarised laser, giving unique information on the sample from a combination of electronic and nuclear properties. In the first instance, such maps can be interpreted empirically, without immediate recourse to theory.

In this paper, systematic development of the semi-classical theory and field applied computer simulation (FMD) of optical NMR is pursued without restriction to samples with a net electronic angular momentum. In section 2 the fundamental semi-classical energy of this theory is given in terms of a mediating molecular property tensor, $(\mathrm{i}\,{}^{\mathrm{m}}\beta''^{\mathrm{ee}}_{ijk})_{mn}$, the imaginary part of a transition magnetic/electric/electric hyperpolarisability which is called the "beta tensor". This is P and T positive and is therefore sustained in chiral and achiral molecular structures. It is also sustained in both diamagnetic and paramagnetic molecules, and its structure is closely similar to the mediating tensor of the Faraday effect [13]. Importantly, therefore, optical NMR is potentially applicable to all atoms and molecules, provided there is a nucleus with a nonvanishing magnetic dipole moment, as in conventional (laser-free) NMR. An order of magnitude estimate of the beta tensor is given, together with the expected broadening in Hz of an NMR spectral line for a given laser intensity I in $\mathrm{W/m^2}$. In section 3 the selection rules associated with beta are given for all molecular point groups for several quantum numbers, including J, the total angular momentum quantum number, M, the magnetic quantum number, which is the projection of J on the Z-axis, and for K, which is the projection of J on an intramolecular symmetry axis. The selection rules are developed in analogy with those governing the transition electric/electric/electric hyperpolarisability tensor mediating hyper-Raman scattering [33,34], and transitions between M levels govern the contribution of $(\mathrm{i}\,\beta''^{\mathrm{ee}}_{ijk})_{mn}$ to the overall optical NMR spectrum. The selection rules for J and M turn out to be

$$\Delta J = 0, \pm 1, \pm 2\,,$$
$$\Delta M = 0, \pm 1, \pm 2\,, \tag{6}$$

for the asymmetric top, leading to a much richer spectrum in optical NMR than in conventional NMR, where the nuclear M selection rule is

$$\Delta M_I = 0, \pm 1\,. \tag{7}$$

In section 4, the perturbation calculus of $(\mathrm{i}\,{}^{\mathrm{m}}\beta''^{\mathrm{ee}}_{ijk})_{mn}$ is derived in semiclassical theory [13] using the matrix density formalism [32], revealing a rich close to optical resonance structure. This implies that tuning the laser to a natural optical resonance frequency of $({}^{\mathrm{m}}\beta''^{ee}_{ijk})_{mn}$ of the sample will profoundly affect the optical NMR spectrum, something which is clearly of practical importance, because the magnitude of beta increases near resonance by as much as about two orders.

In section 5, the point group symmetries and nonvanishing elements of beta in the molecule fixed frame of reference (1, 2, 3) are tabulated for all molecular point groups, in analogy with similar tables in the literature [35] for the closely related mediating tensors of the Faraday effect and the IFE.

In section 6, a field applied molecular dynamics (FMD) computer simulation is pursued using the torque [36–40] set up between the induced transition magnetic dipole moment

$$(m_i^{(\mathrm{ind})})_{mn} = (\mathrm{i}\,{}^{\mathrm{m}}\beta''^{\mathrm{ee}}_{ijk})_{mn}\Pi^{\mathrm{A}}_{jk} \tag{8}$$

and the static magnetic flux density of the permanent magnet. The effect of this torque is worked out classically in terms of orientational rise transients [35,36] and time correlation functions in the statistically stationary state in the presence of both laser and magnet. This provides insight in the classical nature of magnetisation by a circularly polarised laser as mediated by the tensor beta. This approach is roughly analogous to the well known approach based on the Bloch equations of conventional NMR, where the torque is

$$\boldsymbol{T}^{(\mathrm{NMR})} = -\boldsymbol{m}^{(\mathrm{N})} \times \boldsymbol{B}^{(0)}\,. \tag{9}$$

Simulation results are given in terms of a variety of transients and correlation functions for liquid water.

In section 7, orientational functions akin to the Langevin and Kielich [41] functions are given by

thermodynamic averaging over the energy

$$\Delta H_1 = -(\mathrm{i}\,{}^{\mathrm{m}}\beta''^{\mathrm{cc}}_{ijk})_{mn}\Pi^{\mathrm{A}}_{jk}B^{(0)}_i\,, \tag{10}$$

which is the nonvanishing part of the optical NMR energy due to the combined effect of Π^{A}_{jk} and $B^{(0)}_i$ of the laser and magnet, respectively. These are worked out in terms of triple integrals over Euler angles, integrals which are evaluated by a combination of double and single variable numerical quadrature.

Finally, the discussion is devoted to the experimental aspects of the development of optical NMR with conventional two-dimensional, pulse, and Fourier transform NMR spectrometers. A brief discussion is given of the related technique of optical ESR.

2. The optical NMR interaction energy and order of magnitude of the NMR broadening (Hz) for given laser intensity I (W/m^2)

In this paper attention is restricted specifically to the energy

$$\Delta H_2 = -\mathrm{i}({}^{\mathrm{m}}\beta''^{\mathrm{cc}}_{ijk})_{mn}\Pi^{\mathrm{A}}_{jk}B^{(0)}_i - m^{(\mathrm{N})}_i B^{(0)}_i$$
$$= -(\mathrm{i}({}^{\mathrm{m}}\beta''^{\mathrm{cc}}_{ijk})_{mn}\Pi^{\mathrm{A}}_{jk} + m^{(\mathrm{N})}_i)B^{(0)}_i\,, \tag{11}$$

which describes the combined effect of a circularly polarised laser propagating in the same (Z) axis as the magnetic flux density vector, $B^{(0)}_i$, of the permanent magnet of an NMR spectrometer. In eq. (11), Π^{A}_{jk} is the tensor representation (see section 1) of the conjugate product of the laser, $(\mathrm{i}\,{}^{\mathrm{m}}\beta''^{\mathrm{cc}}_{ijk})_{mn}$ is the imaginary part of the rank three molecular property transition tensor beta, $m^{(\mathrm{N})}_i$ is the nuclear magnetic dipole moment. Appendix A gives some further details of how this energy was derived, and relates the beta tensor to the mediating tensor of the Faraday effect and IFE. It is instructive to note several properties of beta from a symmetry consideration of the energy and from the properties of the closely related mediating tensor of the Faraday effect [8].

The order of magnitude of the beta tensor far from optical resonance is 10^{-45} A m^4 V^{-2} [8], an estimate which is based on the mediating tensor [11,41] of the Faraday effect, whose order of magnitude can be derived from literature Verdet constants of diamagnetics such as those listed in tables V and VII in Woźniak et al. [8]. Near optical resonances [41] (see section 4) this may increase to about 10^{-43} A m^4 V^{-2}. The various symmetry relations between the Faraday effect mediating tensor, that of the IFE and our beta tensor are listed in ref. [41]. This order of magnitude for the beta tensor immediately allows a rule of thumb, practical estimate to be made of the magnitude of the extra energy term

$$\Delta H_1 = -\mathrm{i}({}^{\mathrm{m}}\beta''^{\mathrm{cc}}_{ijk})_{mn}\Pi^{\mathrm{A}}_{jk}B^{(0)}_i$$
$$\approx -10^{-45}|\Pi^{\mathrm{A}}_{jk}B^{(0)}_i|\,, \tag{12}$$

set up by the combined effect of laser and magnet. The relation between the scalar electric field strength amplitude (V/m) and the intensity I (W/m^2) of the laser is, in SI units

$$I = \tfrac{1}{2}c\epsilon_0 E_0^2\,, \tag{13}$$

where ϵ_0 is the vacuum permittivity (8.854×10^{-12} J^{-1} C^2 m^{-1}) and c the velocity of light (2.998×10^8 m s^{-1}). Assuming that the flux density of the permanent magnet ($B^{(0)}$) is of the order 10 T, and taking an order of magnitude of 10^{-45} A m^4 V^2 for beta leads to an energy in J from eq. (12) of the order

$$\Delta H_1 \approx -10^{-40} I\ \mathrm{J}\,. \tag{14}$$

The equivalent frequency in Hz is this energy divided by the Planck constant (6.626×10^{-34} J s):

$$\Delta f_1 \approx 1.4\times10^{-7} I\ \mathrm{Hz}\,. \tag{15}$$

Therefore, a laser intensity of 10^7 W m^{-2} (i.e. 10 W/mm^2) will cause a shift in an NMR line of the order of 1.4 Hz from the rule of thumb estimate eq. (15), a shift caused by transitions between M levels of the induced and quantised transition magnetic dipole moment. Note that if the circular polarity of the laser is switched in such a way that the conjugate product vector is changed from parallel to $\boldsymbol{B}^{(0)}$ to anti-parallel, the shift will change direction from the high- to the low-frequency side of the laser-off NMR resonance line. If the laser is not circularly polarised, there should be no effect. These basic considerations are helpful in the removal or isolation of artifacts, due for example to possible heating effects of the laser, or from fluctuations in the laser intensity. This is experimental work currently in progress by Warren et al. [26]. Furthermore, if the laser intensity is increased, the shift should be proportional to I in W/m^2 for constant $\boldsymbol{B}^{(0)}$ and constant laser frequency (usually in

the visible range). Thirdly, for constant I and $\boldsymbol{B}^{(0)}$, the shift should increase as the laser frequency is tuned to an optical resonance of the sample. Finally, the nuclear and optical (i.e. electronic) resonances are linked in general by Landé coupling [18]. The theory of Landé coupling is developed in section 3 of this paper, where selection rules are developed based on the symmetry properties of $(\mathrm{i}\,{}^{\mathrm{m}}\beta''^{\mathrm{ee}}_{ijk})_{mn}$.

The rest of this paper is concerned with a quantum and simplified classical treatment of the shift, and with simulating classically the effect of the laser on the ensemble molecular dynamics in liquid water. This requires a knowledge of the nonvanishing elements of the beta tensor in all the molecular point groups, (section 5), a knowledge of the slection rules between M states allowed by beta, (section 3), and Landé and dipole–dipole coupling between the electronic (laser induced) and nuclear (magnetically induced) parts of the interaction energy, eq. (11). It also requires (section 4) a development of the internal quantum structure of beta. A classical field applied molecular dynamics (FMD) simulation (section 6) of the effect of the laser on the molecular dynamics is also reported.

Of basic importance to the understanding of optical NMR is that the conjugate product Π^{A}_{jk} of the laser induces a quantised magnetic dipole moment, eq. (8), in a diamagnetic or paramagnetic molecule or chromophore. The energy is made up of the interaction between $(\boldsymbol{m}^{(\mathrm{ind})})_{mn}$ and $\boldsymbol{B}^{(0)}$ of the permanent magnet of the NMR spectrometer. Therefore optical NMR works through the *combined* effect of the magnet and circularly polarised laser. For a molecule such as water of C_{2v} symmetry, for example, there are only three independent elements (section 5) of beta in the molecule frame (1, 2, 3). In this frame, the components of the induced magnetic dipole moment can be expressed directly in terms of I (W/m^2) as

$$(m_1^{(\mathrm{ind})})_{mn} = \frac{4e_{1Z}({}^{\mathrm{m}}\beta''^{\mathrm{ee}}_{123})_{mn}I}{(c\epsilon_0)}$$

$$(m_2^{(\mathrm{ind})})_{mn} = \frac{4e_{2Z}({}^{\mathrm{m}}\beta''^{\mathrm{ee}}_{231})_{mn}I}{(c\epsilon_0)}$$

$$(m_3^{(\mathrm{ind})})_{mn} = \frac{4e_{3Z}({}^{\mathrm{m}}\beta''^{\mathrm{ee}}_{312})_{mn}I}{(c\epsilon_0)} \qquad (16)$$

where $\boldsymbol{e}_1$, $\boldsymbol{e}_2$ and $\boldsymbol{e}_3$ are unit vectors in the direction of the axes 1, 2 and 3 showing that the induced magnetic dipole moment is directly proportional to the intensity of the circularly polarised laser. Note that the induced magnetic dipole moment depends on elements of the rank three tensor beta, and as a consequence, the quantum mechanical selection rules between magnetic states (M quantum number) of $(\boldsymbol{m}^{(\mathrm{ind})})_{mn}$ are determined by the way in which beta transforms in the point group $R_h(3)$ of all rotations and reflections of an achiral ensemble [42], or alternatively by the point group R(3) of all rotations of a chiral ensemble. Since $(\boldsymbol{m}^{(\mathrm{ind})})_{mn}$ is a magnetic dipole moment, it is proportional through a T and P positive scalar quantity to an induced and quantised angular momentum, $\boldsymbol{J}^{(\mathrm{ind})}$. This is analogous with the way in which the permanent nuclear magnetic dipole moment is proportional to the net nuclear spin angular momentum through the nuclear gyromagnetic ratio. These statements can be made on the basis of symmetry alone, since magnetic dipole moment and angular momentum are both antisymmetric under T, symmetric under P axial vectors [19].

3. Rotational selection rules, Landé, and dipole–dipole coupling

It is helpful to develop some properties of the transition tensor $(\mathrm{i}\,{}^{\mathrm{m}}\beta''^{\mathrm{ee}}_{ijk})_{mn}$ in close analogy with the classical and quantum treatments of the Raman effect. The polarisability α_{ij} in Raman scattering changes periodically with time if the molecule is rotating or vibrating, or oscillating between electronic or mixed states. (In molecules every electronic transition is accompanied in general by vibrational and rotational transitions.) For pure rotational Raman scattering α_{ij} must vary as the molecule rotates, and for vibrational Raman scattering it varies as the molecule is distorted. The induced electric dipole moment in Raman scattering must oscillate with a superposition of frequencies. It has full spatial quantisation characteristics, and is a quantised, induced, transition electric dipole moment. Associated with it are the well known rotational Raman selection rules

$$\Delta J = 0, \pm 1, \pm 2,$$

$\Delta M = 0, \pm 1, \pm 2$.

The polarisability needed to produce these results can be expressed classically as [6]

$$\alpha_{ij} = \alpha_{0ij} + \Delta\alpha_{ij} \cos \omega_{\mathrm{int}} t ,$$

where ω_{int} is some characteristic frequency of the molecule, which may be rotational, vibrational, electronic, or a mixture. Quantum mechanically, α_{ij} becomes a transition polarisability $(\alpha_{ij})_{mn}$ between quantum states n and m.

In an entirely analogous way, the magnetic dipole moment induced by the interaction (8) between the transition beta tensor and $\hat{\Pi}_{ij}$ must oscillate with a superposition of molecular rotational, vibrational and electronic frequencies. It is therefore fully quantised with selection rules (vide infra)

$\Delta J = 0, \pm 1, \pm 2, \pm 3$,

$\Delta M = 0, \pm 1, \pm 2, \pm 3$.

This induced magnetic dipole moment is coupled to the nuclear magnetic dipole moment in two models: (1) Landé coupling; (2) dipole–dipole coupling. The latter model is particularly easy to understand, because there is a local magnetic field induced at the nucleus by $(m_i^{(\mathrm{ind})})_{mn}$. The local nuclear magnetic field is different from the applied field and there is a chemical shift induced in the NMR spectrum by interaction of the induced and nuclear magnetic dipole moments. This occurs in addition to resonances between M states of the induced magnetic dipole moment itself. The "laser induced shifts" are as useful as the chemical shift which is the basis of conventional NMR.

The rotational selection rules governing the existence of

$$\langle V_{\mathrm{F}} J_{\mathrm{F}} M_{\mathrm{F}} K_{\mathrm{F}} | \Delta H_2 | V_{\mathrm{I}} J_{\mathrm{I}} M_{\mathrm{I}} K_{\mathrm{I}} \rangle$$

are of key importance in optical NMR. Here V_{I} and V_{F} are the initial and final vibrational quantum numbers, and J_{I}, M_{I}, K_{I} and J_{F}, M_{F}, K_{F} the rotational counterparts. As usual [6], J is the total angular momentum quantum number with reference to the laboratory frame (X, Y, Z), M, the magnetic quantum number, governs the Z component of the quantised molecular angular momentum J, and K governs the component of J with reference to an axis, called the principal axis, of the molecule fixed frame (1, 2, 3). We label the principal axis as axis 1.

To derive the selection rules associated with the complete beta tensor of optical NMR it is convenient to work with the irreducible D representations [13,43] of the molecular ensemble in frame (X, Y, Z), and transform when appropriate to frame (1, 2, 3). Recall that the irreducible reresentations of the point group of all rotations and reflections [43], $\mathrm{R_h}(3)$, of achiral ensembles are

$$D_{\mathrm{g}}^{(0)}, D_{\mathrm{g}}^{(1)}, D_{\mathrm{g}}^{(2)}, \ldots, D_{\mathrm{g}}^{(n)}$$

and

$$D_{\mathrm{u}}^{(0)}, D_{\mathrm{u}}^{(1)}, D_{\mathrm{u}}^{(2)}, \ldots, D_{\mathrm{u}}^{(n)} ,$$

respectively, for quantities symmetric and antisymmetric under parity inversion P. In the point group $\mathrm{R}(3)$ of all rotations of a chiral ensemble the irreducible representations are

$$D^{(0)}, D^{(1)}, D^{(2)}, \ldots, D^{(n)} .$$

The totally symmetric irreducible representation (TSR) is that of a scalar quantity such a energy, giving the symmetry representations

$$\Gamma(\langle V_{\mathrm{F}} J_{\mathrm{F}} M_{\mathrm{F}} K_{\mathrm{F}} | \tilde{m}_i^{(N)} | V_{\mathrm{I}} J_{\mathrm{I}} M_{\mathrm{I}} K_{\mathrm{I}} \rangle) ,$$

contains $D_{\mathrm{g}}^{(0)}$,

$$\Gamma(\langle V_{\mathrm{F}} J_{\mathrm{F}} M_{\mathrm{F}} K_{\mathrm{F}} | \mathrm{i}\, {}^{\mathrm{m}}\hat{\beta}_{ijk}^{\mathrm{ncc}} | V_{\mathrm{I}} J_{\mathrm{I}} M_{\mathrm{I}} K_{\mathrm{I}} \rangle) ,$$

contains $D_{\mathrm{g}}^{(0)}$.

Using the Born–Oppenheimer approximation to factorise the vibrational from the rotational quantum numbers, we have

$$\begin{aligned} &\langle V_{\mathrm{F}} J_{\mathrm{F}} M_{\mathrm{F}} K_{\mathrm{F}} | \mathrm{i}\, {}^{\mathrm{m}}\hat{\beta}_{ijk}^{\mathrm{ncc}} | V_{\mathrm{I}} J_{\mathrm{I}} M_{\mathrm{I}} K_{\mathrm{I}} \rangle \\ &\quad \approx \langle V_{\mathrm{F}} | \mathrm{i}\, {}^{\mathrm{m}}\hat{\beta}_{ijk}^{\mathrm{ncc}} | V_{\mathrm{I}} \rangle \\ &\quad + \langle J_{\mathrm{F}} M_{\mathrm{F}} K_{\mathrm{F}} | \mathrm{i}\, {}^{\mathrm{m}}\hat{\beta}_{ijk}^{\mathrm{nee}} | J_{\mathrm{I}} M_{\mathrm{I}} K_{\mathrm{I}} \rangle . \end{aligned} \tag{17}$$

The symmetry representation of the initial total electronic angular momentum wavefunction, $|J_{\mathrm{I}}\rangle$, induced by the laser is [13]

$$\Gamma(|J_{\mathrm{I}}\rangle) = D_{\mathrm{g}}^{(J)} . \tag{18}$$

It follows that for the energy

$$\langle J_{\mathrm{F}} | \mathrm{i}\, {}^{\mathrm{m}}\hat{\beta}_{ijk}^{\mathrm{ncc}} | J_{\mathrm{I}} \rangle$$

to contain the TSR, and therefore not to vanish, the product

$$\Gamma(\langle J_F|\,\mathrm{i}\,{}^{\mathrm{m}}\hat{\beta}''^{\mathrm{ee}}_{ijk})=\Gamma(\langle J_F|\,)\Gamma(\mathrm{i}\,{}^{\mathrm{m}}\hat{\beta}''^{\mathrm{ee}}_{ijk}) \tag{19}$$

must contain $\Gamma(|J_1\rangle)$ at least once. If this is the case, products such as

$$\Gamma(\langle J_F|\,\mathrm{i}\,{}^{\mathrm{m}}\hat{\beta}''^{\mathrm{ee}}_{ijk}|J_1\rangle)$$

automatically generate the TSR, both in achiral and chiral ensembles. In other words the product of an irreducible D representation with itself always contains the TSR. This is the basis of the selection rule governing J that we are seeking.

The symmetry of the complete beta tensor (real and imaginary parts), is the product of the D representations of one magnetic and two electric dipole moments (section 4)

$$\begin{aligned}\Gamma({}^{\mathrm{m}}\beta^{\mathrm{ee}}_{ijk})&=D^{(1)}_{\mathrm{g}}D^{(1)}_{\mathrm{u}}D^{(1)}_{\mathrm{u}}:\mathrm{R_h}(3)\\&=D^{(0)}_{\mathrm{g}}+3D^{(1)}_{\mathrm{g}}+2D^{(2)}_{\mathrm{g}}+D^{(3)}_{\mathrm{g}}:\mathrm{R_h}(3)\\&=D^{(0)}+3D^{(1)}+2D^{(2)}+D^{(3)}:\mathrm{R}(3)\end{aligned} \tag{20}$$

a sum of seven irreducible representations in general, from rank zero (the trace) to rank three. From eq. (19) the product of symmetry representations

$$\begin{aligned}&D^{(1)}_{\mathrm{g}}(D^{(0)}_{\mathrm{g}}+3D^{(1)}_{\mathrm{g}}+2D^{(2)}_{\mathrm{g}}+D^{(3)}_{\mathrm{g}})\\&=D^{(J)}_{\mathrm{g}}+3(D^{(J+1)}_{\mathrm{g}}+D^{(J)}_{\mathrm{g}}+D^{(J-1)}_{\mathrm{g}})\\&+2(D^{(J+2)}_{\mathrm{g}}+\cdots+D^{(J-2)}_{\mathrm{g}})\\&+(D^{(J+3)}_{\mathrm{g}}+\cdots+D^{(J-3)}_{\mathrm{g}})\end{aligned} \tag{21}$$

must contain $D^{(J)}_{\mathrm{g}}$ at least once, and this is possible if and only if

$$\Delta J=0,\ \pm1,\ \pm2,\ \pm3\,. \tag{22}$$

Note that we have used the Clebsch–Gordan theorem [6] to work out products of D representations

$$D^{(J)}_{\mathrm{g}}D^{(n)}_{\mathrm{g}}=D^{(J+n)}_{\mathrm{g}}+\cdots+D^{|J-n|}_{\mathrm{g}}\,. \tag{23}$$

Eq. (22) represents the selection rule on the complete tensor beta. To find the J selection rules governing the imaginary part of beta appearing in the optical NMR Hamiltonian recall that $(\mathrm{i}\,\beta''^{\mathrm{ee}}_{ijk})_{mn}$ is symmetric under T, and that the real part, $({}^{\mathrm{m}}\beta''^{\mathrm{ee}}_{ijk})_{mn}$, is antisymmetric under T. From this consideration and from the general definitions [6,13,35]

$$\begin{aligned}(\mathrm{i}\,{}^{\mathrm{m}}\beta''^{\mathrm{ee}}_{ijk})&=-[\partial H/(\partial\Pi^{\mathrm{A}}_{ij}\,\partial B^{0}_{k})]_{00}\,,\\({}^{\mathrm{m}}\beta''^{\mathrm{ee}}_{ijk})&=-[\partial H/(\partial\Pi^{\mathrm{S}}_{ij}\,\partial B^{(0)}_{k})]_{00}\,.\end{aligned} \tag{24}$$

where Π^{S}_{ij} is the symmetric part of the conjugate product

$$\Pi^{\mathrm{S}}_{ij}=E_iE^*_i+\tfrac{1}{2}(E_iE^*_j+E_jE^*_i)_{i\neq j}\,. \tag{25}$$

We have

$$\Gamma(\mathrm{i}\,{}^{\mathrm{m}}\beta''^{\mathrm{ee}}_{ijk})=D^{(1)}_{\mathrm{g}}D^{(1)}_{\mathrm{g}}=D^{(0)}_{\mathrm{g}}+D^{(1)}_{\mathrm{g}}+D^{(2)}_{\mathrm{g}}\,, \tag{26}$$

$$\Gamma({}^{\mathrm{m}}\beta''^{\mathrm{ee}}_{ijk})=(D^{(0)}_{\mathrm{g}}+D^{(2)}_{\mathrm{g}})D^{(1)}_{\mathrm{g}}=2D^{(1)}_{\mathrm{g}}+D^{(2)}_{\mathrm{g}}+D^{(3)}_{\mathrm{g}}\,, \tag{27}$$

i.e. the imaginary part of beta is made up of a total of three irreducible representations, of ranks one, two, and three, which are all symmetric under T and P. (The real part of beta, not considered in this paper, is made up of two rank one, one rank two, and one rank three, antisymmetric under T, symmetric under P positive, irreducible representations.) Selection rules on $(\mathrm{i}\,{}^{\mathrm{m}}\beta''^{\mathrm{ee}}_{ijk})_{mn}$ are therefore obtained from the product

$$D^{(J)}_{\mathrm{g}}(D^{(0)}_{\mathrm{g}}+D^{(1)}_{\mathrm{g}}+D^{(2)}_{\mathrm{G}})$$

and are:

$$\Delta J=0,\ \pm1,\ \pm2 \tag{28}$$

from the Clebsch–Gordan theorem governing products of D representations both in $\mathrm{R_h}(3)$ and in $\mathrm{R}(3)$. The selection rules governing the real part of the beta tensor are coincidentally the same as those governing the complete tensor.

It is well known that for each quantum number J there are $(2J+1)$ quantum numbers M

$$-J,\ldots,J\,,$$

and transitions between these M levels (the magnetic, or Zeeman, levels) are of prime interest in optical NMR. Selection rules on M follow from the fact that M is the quantum number associated with the Z-component of the total angular momentum $\boldsymbol{J}$. The D symmetry of the Z-component is the same as that of the complete vector J, and it follows that the M selection rules must be

$$\Delta M=0,\ \pm1,\ \pm2\,. \tag{29}$$

The complete set of M and J selection rules associated with $(\mathrm{i}\,{}^{\mathrm{m}}\beta''^{\mathrm{ee}}_{ijk})_{mn}$ for an asymmetric top molecule is therefore

$$\Delta J = 0, \pm 1, \pm 2 ,$$

$$\Delta M = 0, \pm 1, \pm 2 . \tag{30}$$

The corresponding rules for the real part are

$$\Delta J = 0, \pm 1, \pm 2, \pm 3 ,$$

$$\Delta M = 0, \pm 1, \pm 2, \pm 3 . \tag{31}$$

3.1. Landé coupling and optical NMR transitions

Write the induced magnetic dipole moment as

$$(m_i^{(\mathrm{ind})})_{mn} = -\gamma_{\mathrm{e}}^{(\mathrm{ind})} J_i^{(\mathrm{ind})} = \mathrm{i}({}^{\mathrm{m}}\beta''^{\mathrm{ee}}_{ijk})_{mn} \Pi^{\mathrm{A}}_{jk} , \tag{32}$$

where $\gamma_{\mathrm{e}}^{(\mathrm{ind})}$ is an electronic scalar property and $J_i^{(\mathrm{ind})}$ is the electronic angular momentum induced by Π^{A}_{jk} of the circularly polarised laser, then

$$\Delta H_2 = -(\gamma_{\mathrm{e}}^{(\mathrm{ind})} J_i^{(\mathrm{ind})} + \gamma_{\mathrm{N}} I_i) B_i^{(0)} . \tag{33}$$

Here γ_{N} is the nuclear gyromagnetic ratio [6] and I_i the nuclear spin angular momentum. The quantity $J_i^{(\mathrm{ind})}$ has a quantised operator equivalent obeying the usual fundamental rules of quantum mechanics [6]

$$[J_X^{(\mathrm{ind})}, J_Y^{(\mathrm{ind})}] = \mathrm{i}\hbar J_Z^{(\mathrm{ind})} , \tag{34a}$$

$$[J^{(\mathrm{ind})2}, J_q] = 0 , \tag{34b}$$

$$J^{(\mathrm{ind})2} | J^{(\mathrm{ind})}, M_J^{(\mathrm{ind})} \rangle = J^{(\mathrm{ind})}(J^{(\mathrm{ind})}+1) | J^{(\mathrm{ind})}, M_J^{(\mathrm{ind})} \rangle , \tag{34c}$$

$$J_Z^{(\mathrm{ind})} | J^{(\mathrm{ind})}, M_J^{(\mathrm{ind})} \rangle = M_J^{(\mathrm{ind})} \hbar | J^{(\mathrm{ind})}, M_J^{(\mathrm{ind})} \rangle , \tag{34d}$$

$$M_J^{(\mathrm{ind})} = J^{(\mathrm{ind})}, J^{(\mathrm{ind})}-1, \ldots, -J^{(\mathrm{ind})} . \tag{34e}$$

There is Landé coupling [6,44] between the electronic $J_i^{(\mathrm{ind})}$ and the nuclear I_i. This can be developed theoretically [6] by writing, in vector notation

$$\boldsymbol{J}^{(\mathrm{ind})} \cdot \boldsymbol{B}^{(0)} = \frac{\boldsymbol{J}^{(\mathrm{ind})} \cdot \boldsymbol{J}^{(\mathrm{tot})} \boldsymbol{J}^{(\mathrm{tot})} \cdot \boldsymbol{B}^{(0)}}{(|\boldsymbol{J}^{(\mathrm{tot})}|^2)} , \tag{35a}$$

$$\boldsymbol{I} \cdot \boldsymbol{B}^{(0)} = \frac{\boldsymbol{I} \cdot \boldsymbol{J}^{(\mathrm{tot})} \boldsymbol{J}^{(\mathrm{tot})} \cdot \boldsymbol{B}^{(0)}}{(|\boldsymbol{J}^{(\mathrm{tot})}|^2)} , \tag{35b}$$

$$\boldsymbol{J}^{(\mathrm{tot})} = \boldsymbol{J}^{(\mathrm{ind})} + \boldsymbol{I} . \tag{35c}$$

Using

$$2\boldsymbol{J}^{(\mathrm{ind})} \cdot \boldsymbol{J}^{(\mathrm{tot})} = \boldsymbol{J}^{(\mathrm{tot})2} + \boldsymbol{J}^{(\mathrm{ind})2} - |\boldsymbol{J}^{(\mathrm{tot})} - \boldsymbol{J}^{(\mathrm{ind})}|^2 = \boldsymbol{J}^{(\mathrm{tot})2} + \boldsymbol{J}^{(\mathrm{ind})2} - \boldsymbol{I}^2 , \tag{36a}$$

$$2\boldsymbol{I} \cdot \boldsymbol{J}^{(\mathrm{tot})} = \boldsymbol{J}^{(\mathrm{tot})2} + \boldsymbol{I}^2 - \boldsymbol{J}^{(\mathrm{ind})2} \tag{36b}$$

we obtain the interaction energy ΔH_2 in Landé form

$$\Delta H_2 = \frac{-(\gamma_{\mathrm{e}}^{(\mathrm{ind})} \boldsymbol{J}^{(\mathrm{ind})} \cdot \boldsymbol{J}^{(\mathrm{tot})} + \gamma_{\mathrm{N}} \boldsymbol{I} \cdot \boldsymbol{J}^{(\mathrm{tot})})}{|\boldsymbol{J}^{(\mathrm{tot})2}|} \boldsymbol{J}^{(\mathrm{tot})} \cdot \boldsymbol{B}^{(0)} \equiv -g_{\mathrm{L}} \boldsymbol{J}^{(\mathrm{tot})} \cdot \boldsymbol{B}^{(0)} , \tag{37}$$

$$\Delta M^{(\mathrm{ind})} = 0, \pm 1, \pm 2 ,$$

$$\Delta M_I = 0, \pm 1 ,$$

$$M^{(\mathrm{tot})} = M^{(\mathrm{ind})} + M_I ,$$

where

$$g_{\mathrm{L}} = [\gamma_{\mathrm{e}}^{(\mathrm{ind})} (J^{(\mathrm{tot})}(J^{(\mathrm{tot})}+1) + J^{(\mathrm{ind})}(J^{(\mathrm{ind})}+1) - I(I+1)) + \gamma_{\mathrm{N}} (J^{(\mathrm{tot})}(J^{(\mathrm{tot})}+1) + I(I+1) - J^{(\mathrm{ind})}(J^{(\mathrm{ind})}+1))] / [J^{(\mathrm{tot})}(J^{(\mathrm{tot})}+1)]$$

is the Landé factor.

The total magnetic quantum number is fixed by well known fundamental properties [6,44]

$$M^{(\mathrm{tot})} = M^{(\mathrm{ind})} + M_I . \tag{38}$$

However, we have

$$\Delta M^{(\mathrm{ind})} = 0, \pm 1, \pm 2 , \tag{39}$$

so that for a given M_I, the sum $M^{(\mathrm{tot})}$ can change by 0, ± 1, ± 2, ± 3. The selection rule for $M^{(\mathrm{tot})}$ is therefore

$$\Delta M^{(\mathrm{tot})} = 0, \pm 1, \pm 2, \pm 3 . \tag{40}$$

The Landé factor is constant for a given $J^{(\mathrm{tot})}$, independent of $M^{(\mathrm{tot})}$, so the optical NMR beta theory of this paper is similar to the well known problem of computing the Zeeman effect of free atoms, described well by Townes and Schawlow [45], and in which there is coupling of orbital and spin electronic angular momenta. In the beta theory of optical NMR, there is coupling of a laser induced angular momentum, $J^{(\mathrm{ind})}$, and the nuclear spin angular momentum, I. (For a beta theory of optical ESR, replace I by the electronic spin angular momentum and the nuclear by the electronic gyromagnetic ratio.)

From eq. (37) the NMR transition frequencies in rad/s (observable optical NMR lines) are given by

$$\omega_2 = \frac{(\Delta H_2)_{F\leftarrow I}}{\hbar}$$

$$= (g_{L1} M_1^{(\mathrm{tot})} - g_{L2} M_2^{(\mathrm{tot})}) B_Z^{(0)} , \quad \omega_2 \geq 0 , \qquad (41)$$

with the transitions between magnetic quantum levels governed by

$$\Delta M^{(\mathrm{tot})} = M_1^{(\mathrm{tot})} - M_2^{(\mathrm{tot})} = 0, \pm 1, \pm 2, \pm 3 . \qquad (42)$$

In order to obtain an order of magnitude estimate of the electronic scalar property $\gamma_e^{(\mathrm{ind})}$ we use the equivalence of quantum and semiclassical descriptions

$$\frac{1}{\hbar}(\mathrm{i}({}^{\mathrm{m}}\beta''^{\mathrm{ee}}_{Zjk})_{mn} \Pi^{\mathrm{A}}_{jk} - m_Z^{(\mathrm{N})})_{F\leftarrow I}$$

$$= (g_{L1} M_1^{(\mathrm{tot})} - g_{L2} M_2^{(\mathrm{tot})}) . \qquad (43)$$

Here $(g_{L1} M_1 - g_{L2} M_2)$ is a number of the order one, so that the order of magnitude of $\gamma_e^{(\mathrm{ind})}$ is

$$\gamma_e^{(\mathrm{ind})} \approx \left(\frac{\mathrm{i}({}^{\mathrm{m}}\beta''^{\mathrm{ee}}_{Zjk})_{mn} \Pi^{\mathrm{A}}_{jk}}{\hbar} \right) \gamma_e \approx 10^{-11} |\Pi^{\mathrm{A}}_{jk}| \gamma_e , \qquad (44)$$

which depends on $|\Pi^{\mathrm{A}}_{jk}|$. Note that this multiplies the gyromagnetic ratio of the electron, whose order of magnitude is SI is $\gamma_e = 9.3 \times 10^{10}$ C kg m^{-1}.

Eq. (41) is of direct use in computing the optical NMR spectrum, the way in which the circularly polarised laser splits the conventional NMR spectrum. The allowed angular momentum states of the split spectrum are

$$J^{(\mathrm{ind})} + I; J^{(\mathrm{ind})} + I - 1; \ldots; |J^{(\mathrm{ind})} - I| ;$$

and the coupling of these states has been treated through Landé theory in deriving the rule (41). More generally, the coupled and uncoupled representations [6,41] apply to the quantum mechanical description of how $\boldsymbol{J}^{(\mathrm{ind})}$ interacts with $\boldsymbol{I}$ to give an optical NMR spectrum consisting of many more lines than the conventional NMR spectrum. In the coupled representation [6,44] the coupled state is built up in general from the two states $|IM_I\rangle$ and $|J^{(\mathrm{ind})} M^{(\mathrm{ind})}\rangle$. This can be represented in standard notation [44] by

$$|J^{(\mathrm{ind})} I J^{(\mathrm{tot})} M^{(\mathrm{tot})}\rangle$$

$$= \sum_{M^{(\mathrm{ind})}, M_I} \langle J^{(\mathrm{ind})} M^{(\mathrm{ind})}, I M_I | J^{(\mathrm{tot})} M^{(\mathrm{tot})} \rangle$$

$$\times |J^{(\mathrm{ind})} M^{(\mathrm{ind})}\rangle |IM_I\rangle$$

$$= \sum_{M^{(\mathrm{ind})}, M_I} (-1)^{J^{(\mathrm{ind})} - I + M^{(\mathrm{tot})}} (2J^{(\mathrm{tot})} + 1)^{1/2}$$

$$\times \begin{pmatrix} J^{(\mathrm{ind})} & I & J^{(\mathrm{tot})} \\ M^{(\mathrm{ind})} & M_I & -M^{(\mathrm{tot})} \end{pmatrix} |J^{(\mathrm{ind})} M^{(ind)}\rangle |IM_I\rangle , \qquad (45)$$

where we have also used the standard notation [44] for the Clebsch–Gordan coefficients and 3-j symbol. The former is conveniently computed through [44]

$$\langle j_1 m_1, j_2 m_2 | j_3 m_3 \rangle$$

$$= \delta_{m_1 + m_2, m_3} [(2j_3 + 1) \frac{(s-2j_3)!(s-2j_2)!(s-2j_1)!}{(s+1)!}$$

$$\times (j_1 + m_1)!(j_1 - m_1)!(j_2 + m_2)!(j_2 - m_2)!(j_3 + m_3)!$$

$$\times (j_3 - m_3)!]^{1/2}$$

$$\times \sum_{\nu} (-1)^{\nu} / [\nu!(j_1 + j_2 - j_3 - \nu)!(j_1 - m_1 - \nu)!$$

$$\times (j_2 + m_2 - \nu)!(j_3 - j_2 + m_1 + \nu)!$$

$$\times (j_3 - j_1 - m_2 + \nu)!] , \qquad (46)$$

where

$$s = j_1 + j_2 + j_3 \qquad (47)$$

and the index ν ranges over all integral values for which the factorial arguments are non-negative. The Clebsch–Gordan coefficient vanishes unless

$$m_3 = m_1 + m_2 , \qquad (48)$$

which gives the rule (38) used previously.

The coupled representation $|J^{(\mathrm{tot})} M^{(\mathrm{tot})}\rangle$ in general is represented by a precession of the $\boldsymbol{J}^{(\mathrm{ind})}$ and $\boldsymbol{I}$ vectors in phase [44] about the resultant $\boldsymbol{J}^{(\mathrm{tot})}$, which itself precesses about the propagation axis Z of the laboratory frame. The Clebsch–Gordan coefficient is a number expressing the probability [44] amplitude that the coupled state $|J^{(\mathrm{tot})} M^{(\mathrm{tot})}\rangle$ will be found having its component parts $J^{(\mathrm{ind})}$ and I making the projections $M^{(\mathrm{ind})}$ and M_I for $J_Z^{(\mathrm{ind})}$ and I_Z, respectively. The 3-J symbol, also widely used in the literature, is this divided by $(2J^{(\mathrm{tot})} + 1)^{1/2}$. The Clebsch–

Gordan coefficient is also the probability amplitude that the uncoupled state $|J^{(ind)}M^{(ind)}, IM_I\rangle$ at any instant couples to form a resultant state $|J^{(tot)}M^{(tot)}\rangle$ of length $(J^{(tot)}(J^{(tot)}+1))^{1/2}$. The square of the Clebsch–Gordan coefficient is a proper fraction [44] whose value ranges from 0 to 1. As usual, the uncoupled and coupled representations are equivalent [6] descriptions of the same physical process of interaction between $\boldsymbol{J}^{(ind)}$ and $\boldsymbol{I}$. In the uncoupled representation, $\boldsymbol{J}^{(ind)}$ and $\boldsymbol{I}$ precess independently.

To summarise this section, it is clear from eq. (41) that the circularly polarised laser splits a conventional NMR line into several different lines, governed by the quantum numbers

$$J^{(ind)}+I, \ldots, |J^{(ind)}-I| , \tag{49}$$

arising from coupling between the laser induced electronic $\boldsymbol{J}^{(ind)}$ and the nuclear $\boldsymbol{I}$. Optical NMR therefore depends on the electronic environment much more markedly than conventional NMR.

Transitions between the levels (49) are governed by the selection rules

$$M_1^{(tot)} - M_2^{(tot)} = \Delta M^{(tot)} = 0, \pm 1, \pm 2, \pm 3 ,$$

giving a rich variety of spectral detail if resolved experimentally. The spacing between these lines depends on the laser intensity and the flux density of the permanent NMR magnet through the coefficient $\gamma_e^{(ind)}$ and the nuclear gyromagnetic ratio. The quantity $\gamma_e^{(ind)}$ is related to the beta tensor through eq. (44).

This is enough information for an experimental assessment of the beta theory, in particular an attempt at resolving the broadening predicted by the rule of thumb estimate in section 2.

A specific example of the effect of Landé coupling is shown in fig. 1 using eq. (37) with the specific quantum transitions

$$I_f = 0.5 , \quad I_i = 0.5 , \quad M_{I_f} = 0.5 , \quad M_{I_i} = -0.5 ,$$

$$J_i^{(ind)} = 1 , \quad M_i^{(ind)} = -1 ,$$

$$J_f^{(ind)} = 1 , \quad M_f^{(ind)} = 1 ,$$

$$J_f^{(tot)} = J_f^{(ind)} + I_f , \quad J_i^{(tot)} = J_i^{(ind)} + I_i ,$$

$$M_f^{(tot)} = M_f^{(ind)} + M_{I_f} , \quad M_i^{(tot)} = M_i^{(ind)} + M_{I_i} .$$

In fig. 1 the product $\gamma_N B_Z^{(0)}$ is normalised to one, and the laser intensity on the abscissa is measured in terms of the ratio $\gamma_e^{(ind)}/\gamma_N$. The ordinate gives the normalised resonance frequency, and this is seen to increase with laser intensity for the particular optical NMR line considered. This implies that some optical NMR lines are shifted considerably to higher frequency in relation to their conventional NMR counterparts, and the absolute frequency separation between such lines is also increased, something which is potentially useful in the resolution of spectra with many lines.

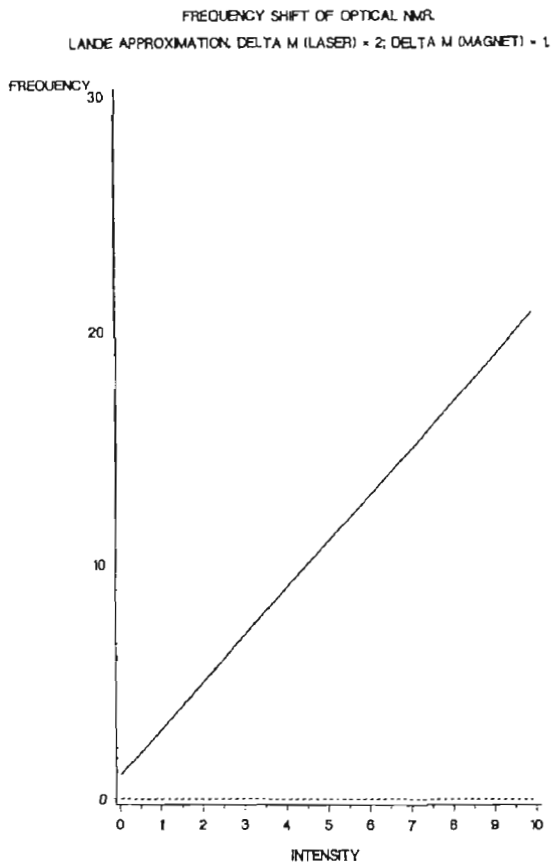

Fig. 1. — Laser shift due to Landé coupling, --- baseline (no laser).

3.2. Dipole–dipole model

The complexities of the foregoing quantum description can be bypassed with the appealing dipole–dipole model perturbation Hamiltonian

$$H_{mm} = -\boldsymbol{m}_N \cdot \boldsymbol{B} - \boldsymbol{m}^{(ind)} \cdot \boldsymbol{B} + \lambda \boldsymbol{m}_N \cdot \boldsymbol{m}^{(ind)} ,$$

which implies, as in the theory of the chemical shift, that there is a local quantised electronic magnetic dipole moment, $\boldsymbol{m}^{(ind)}$, induced by the laser. This induced magnetic dipole moment produces a magnetic field $\boldsymbol{B}^{(ind)}$ at the nucleus

$$\boldsymbol{B}^{(\mathrm{ind})} = -\left(\frac{\mu_0}{4\pi r^3}\right)(\boldsymbol{m}^{(\mathrm{ind})} - 3\hat{\boldsymbol{r}}\hat{\boldsymbol{r}}\cdot\boldsymbol{m}^{(\mathrm{ind})})$$

where $\hat{\boldsymbol{r}}$ is the unit vector joining the two dipoles $\boldsymbol{m}^{(\mathrm{ind})}$ and $\boldsymbol{m}_{\mathrm{N}}$, and μ_0 is the permeability in vacuo. Therefore the local magnetic field at the nucleus differs from the applied field and it is immediately clear that there is a chemical shift induced by the laser – the "laser shift". In general $\boldsymbol{m}^{(\mathrm{ind})}$ is quantised, but can be treated in its classical limit in this dipole–dipole model. The laser shift is different in general from chromophore to chromophore, since $\boldsymbol{m}^{(\mathrm{ind})}$ is clearly an electronic property with electronic, vibrational and rotational quantum levels. This implies that the laser shift is as useful in principle as the chemical shift, which is the basis of NMR spectroscopy.

4. The beta tensor close to optical resonance

One of the potentialities of optical NMR is its ability to show the response of a sample to tuning the pump laser frequency close to an optical resonance of beta. In this section we adapt the recent work of Woźniak et al. [41] on the close to resonance properties of the IFE and inverse magnetochiral birefringence [12]. In that work, expressions were derived using the matrix density formalism and perturbation calculus in terms of broadening parameters, and it was shown that the IFE and inverse magnetochiral spectra have a variety of close to resonance bandshapes. Importantly, near resonance the magnitude of the beta tensor of the IFE may increase by several orders. This implies that a similar effect is expected in optical NMR, because of the close relations between the tensors demonstrated in ref. [41].

From the matrix density formalism [32], the most general form of the beta tensor of optical NMR is shown in ref. [41]. It can also be derived from Feynman diagrams as shown in ref. [41]. Both methods lead to a close to resonance structure which can be controlled by broadening parameters. The optical NMR tensor beta therefore varies in magnitude as a function of frequency as illustrated in fig. 2. If the circularly polarised laser frequency is tuned to one of these optical resonances (peaks in the beta spectrum) there will be, in theory, a large effect on the optical NMR spectrum, because the effective magnitude of beta at the circularly polarised laser frequency may increase dramatically, depending on the conditions. The effect will show up in an uresolved optical NMR spectrum through the rule of thumb eq. (15), i.e. the broadening in the conventional nuclear magnetic resonance line will increase for a constant $B_2^{(0)}$ following the contours of fig. 2.

5. The molecular and crystallographic point group symmetry of beta, vibrational selection rules and character tables

In this section the properties of the beta tensor of optical NMR are tabulated in the molecular point groups, thirty-two of which are also the crystallographic point groups [46]. This task is made much easier through the relations [11] between the beta tensors of optical NMR and the Faraday effect, so that the tables drawn up by Woźniak et al. [8] can be adapted straightforwardly. We first tabulate the nonvanishing elements of beta in all the molecular point groups, tables 1 and 2. Further symmetry relations such as

$$(\mathrm{i}\,{}^{\mathrm{m}}\beta''^{\mathrm{ee}}_{ijk})_{mn} = -(\mathrm{i}\,{}^{\mathrm{m}}\beta''^{\mathrm{ee}}_{ikj})_{mn} \qquad (50)$$

reduce the number of independent scalar elements in these tables, which are expressed in terms of the frame (1, 2, 3) of the point group. For example in water (point group C_{2v}) the dipole axis is axis 1. The same notation is used as that of Woźniak et al. [8] for the Faraday effect (table IV of ref. [8]). As in Woźniak et al. [8], each of the beta subscripts can take the values 1, 2, or 3 in tables 1 and 2.

For example, for a chiral D_2 point group and achiral C_{2v} point group the 27 possible scalar elements of beta reduce to three, using the fact that beta is antisymmetric in the exchange of two subscripts

$$({}^{\mathrm{m}}\beta''^{\mathrm{ee}}_{123})_{mn} = -({}^{\mathrm{m}}\beta''^{\mathrm{ee}}_{132})_{mn},$$

$$({}^{\mathrm{m}}\beta''^{\mathrm{ee}}_{231})_{mn} = -({}^{\mathrm{m}}\beta''^{\mathrm{ee}}_{213})_{mn},$$

$$({}^{\mathrm{m}}\beta''^{\mathrm{ee}}_{321})_{mn} = -({}^{\mathrm{m}}\beta''^{\mathrm{ee}}_{312})_{mn}.$$

These three elements have been used in deriving eqs. (16) of this paper. In a T_{d} symmetry spherical top molecule such as methane, the beta tensor has only one independent scalar element. The point group properties of the beta tensor of optical NMR are

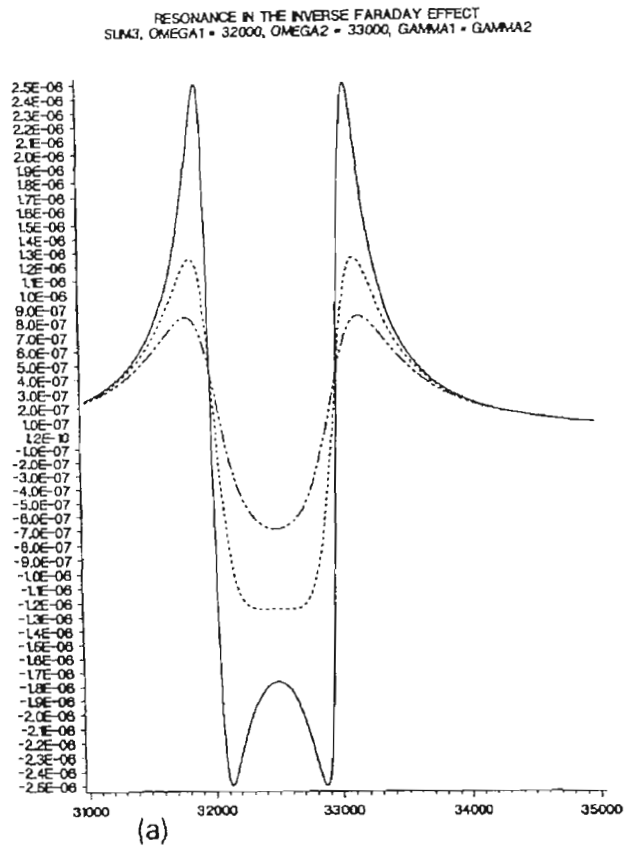

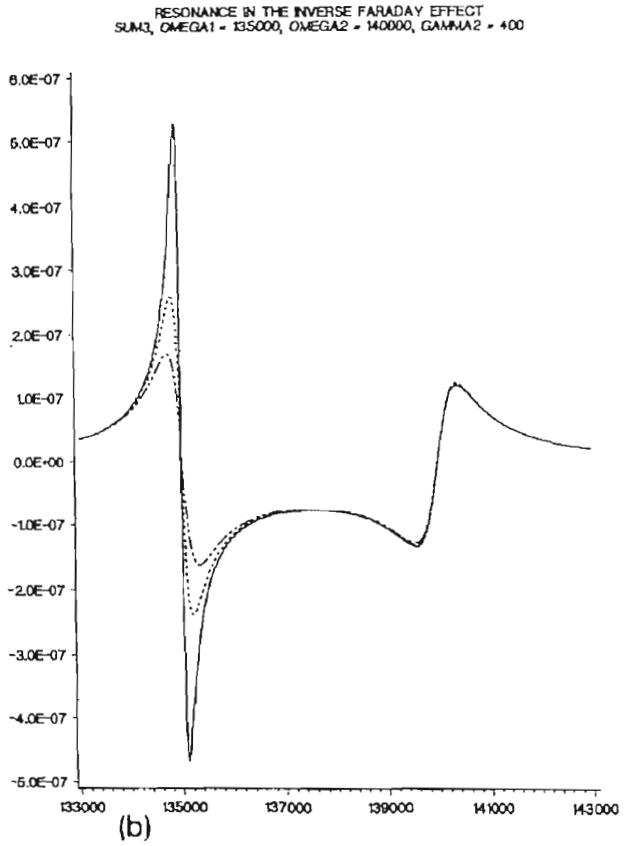

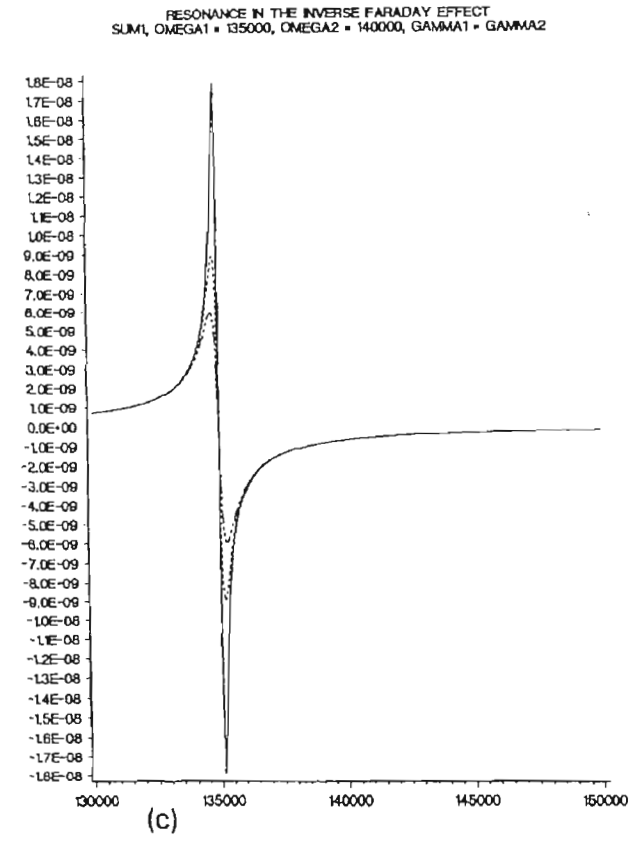

Fig. 2. Some examples of the resonance properties of the optical NMR and inverse Faraday effect tensor (see ref. [4]).

Table 1
Third rank tensor axial optical NMR tensor ${}^{m}\beta''^{cc}_{\alpha\beta\gamma}(0;\omega,-\omega)$. The components of this tensor in some molecular point groups, denoted by the subscripts $\alpha\beta\gamma$: each of which can take the values 1, 2 and 3 of the symmetry frame (1, 2, 3) of the molecule

Point group	${}^{m}\beta''^{cc}_{\alpha\beta\gamma}(0;\omega,-\omega)$
C_1, S_2	$131=-113, 232=-223, 121=-112,$ $313=-331, 212=-221, 323=-332,$ $123=-132, 231=-213, 312=-321.$
C_2, C_{1h}, C_{2h}	$131=-113, 232=-223,$ $123=-132, 231=-213, 312=-321.$
C_{2v}, D_2, D_{2h}	$123=-132, 231=-213, 312=-321.$
C_3, C_{3h}, S_4, C_4, C_{4h}, S_6, C_6, C_{6h}	$131=232=-113=-223,$ $123=231=-132=-213,$ $312=-321.$
D_3, D_4, D_6, D_{2d}, D_{3d}, C_{3v}, C_{4v}, C_{6v}, D_{3h}, D_{4h}, D_{6h}.	$123=231=-132=-213,$ $312=-321.$
T, T_h, T_d, O, O_h, Y, Y_h, K, K_h	$123=231=312=-132=-213=-321$

Table 2
As table 1, linear molecules

Point group	${}^{m}\beta''^{cc}_{\alpha\beta\gamma}(0;\omega,-\omega)$
C_∞, $C_{\infty h}$	$131=232=-113=-223,$ $123=231=-132=-213,$ $312=-321.$
$C_{\infty v}$, $D_{\infty h}$	$123=231=-132=-213,$ $312=-321.$

closely related to those of the Faraday effect and identical with those of the IFE.

The next stage in the development of beta in the molecular point groups is its reduction in terms of irreducible representations [6]. This is given in table 3 for the relevant imaginary part of beta for the thirty-two point groups which happen also to be the crystallographic point groups. This table can be used for the selection rules governing the beta active vibrational modes, whose irreducible representations are given in column 3, and compared with the regular infrared active vibrational modes given in column 4. It is well known [6] that the irreducible representations in column 4 of table 3 are selection rules for infrared active vibrational transitions according to the fact that

$$\langle\mu\rangle_{\nu'\nu''}=\int\Psi^{*}_{\nu'}\mu\Psi_{\nu''}\,d\tau \tag{51}$$

exists [47] if

$$\Gamma(\Psi^{*}_{\nu'})\Gamma(\mu)\Gamma(\Psi_{\nu''})=\Gamma_{IR} \tag{52}$$

contains the totally symmetric irreducible representation (TSR) of the molecular point group at least once. In eq. (51), μ is the transition electric dipole moment and $\Psi_{\nu''}$ and $\Psi^{*}_{\nu'}$ are initial and final vibrational wave functions, which can be represented as combinations of irreducible representations. Analogously, the beta tensor of optical NMR also has vibrational character, which may put an imprint on the optical NMR spectrum through vibration rotation coupling. The vibrational spectrum is governed by the fact that

$$\langle i\,{}^{m}\beta''^{cc}_{ijk}\rangle_{\nu'\nu''}=i\int\Psi^{*}_{\nu'}({}^{m}\beta''^{cc}_{ijk})\Psi_{\nu''}\,d\tau \tag{53}$$

may be non-zero if

$$\Gamma(\Psi^{*}_{\nu'})\Gamma({}^{m}\beta''^{ee}_{ijk})\Gamma(\Psi_{\nu''})=\Gamma_{ONMR} \tag{54}$$

contains the TSR of the molecular point group at least once.

Table 4 is the equivalent of table 3 for the point groups of molecules of linear symmetry, chiral and achiral, and both of these tables can be used to determine the beta active optical NMR modes for a given

Table 3
Irreducible representations (Γ) and active modes of the optical NMR beta tensor in the thirty-two crystallographic point groups, and comparison with infrared active modes

Point group	$\Gamma(i^m\beta''^{cc}_{ijk})$	Active modes	
		beta	infrared
$C_1(1)$	$9A$	A	A
$C_i(S_2)(\bar{1})$	$9A_g$	A_g	A_g
$C_2(2)$	$5A+4B$	A, B	A, B
$C_{1h}(m)$	$5A'+4A''$	A', A''	A', A''
$C_{2h}(2/m)$	$5A_g+4B_g$	A_g, B_g	A_u, B_u
$C_{2v}(2mm)$	$3A_1+2B_1+2B_2+2A_2$	A_1, B_1, B_2, A_2	A_1, B_1, B_2
$D_2(232)$	$3A_1+2B_1+2B_2+2B_3$	A_1, B_1, B_2, B_3	B_1, B_2, B_3
$D_{2h}(mmm)$	$3A_{1g}+2B_{1g}+2B_{2g}+2B_{3g}$	$A_{1g}, B_{1g}, B_{2g}, B_{3g}$	B_{1u}, B_{2u}, B_{3u}
$C_3(3)$	$3A+3E$	A, E	A, E
$C_{3v}(3m)$	$2A_1+A_2+3E$	A_1, A_2, E	A_1, E
$D_3(32)$	$2A_1+A_2+3E$	A_1, A_2, E	A_2, E
$D_{3d}(\bar{3}m)$	$2A_{1g}+A_{2g}+3E_g$	A_{1g}, A_{2g}, E_g	A_{2u}, E_u
$S_6(\bar{3})$	$3A_g+3E_g$	A_g, E_g	A_u, E_u
$C_4(4)$	$3A+2B+2E$	A, B, E	A, E
$C_{4v}(4mm)$	$2A_1+A_2+B_1+B_2+2E$	A_1, A_2, B_1, B_2, E	A_1, E
$C_{4h}(4/m)$	$3A_g+2B_g+2E_g$	A_g, B_g, E_g	A_u, E_u
$D_4(422)$	$2A_1+A_2+B_1+B_2+2E$	A_1, A_2, B_1, B_2, E	A_2, E
$D_{4h}(4/mmm)$	$2A_{1g}+A_{2g}+B_{1g}+B_{2g}+2E_g$	$A_{1g}, A_{2g}, B_{1g}, B_{2g}, E_g$	A_{2u}, E_u
$D_{2d}(\bar{4}2m)$	$2A_1+A_2+B_1+B_2+2E$	A_1, A_2, B_1, B_2, E	B_2, E
$S_4(\bar{4})$	$3A+2B+2E$	A, B, E	B, E
$C_6(6)$	$3A+2E_1+E_2$	A, E_1, E_2	A, E_1
$C_{6v}(6mm)$	$2A_1+A_2+2E_1+E_2$	A_1, A_2, E_1, E_2	A_1, E_1
$C_{3h}(\bar{6})$	$3A'+2E''+E'$	A', E'', E'	A'', E'
$C_{6h}(6/m)$	$3A_g+2E_{1g}+E_{2g}$	A_g, E_{1g}, E_{2g}	A_u, E_{1u}
$D_6(622)$	$2A_1+A_2+E_2+2E_1$	A_1, A_2, E_2, E_1	A_2, E_1
$D_{3h}(6m2)$	$2A_1'+A_2'+E'+2E''$	A_1', A_2', E', E''	A_2'', E'
$D_{6h}(6/mmm)$	$2A_{1g}+A_{2g}+2E_{1g}+E_{2g}$	$A_{1g}, A_{2g}, E_{1g}, E_{2g}$	A_{2u}, E_{1u}
$T_d(\bar{4}3m)$	$A_1+T_1+E+T_2$	A_1, T_1, E, T_2	T_2
$O_h(m3m)$	$A_{1g}+T_{1g}+E_g+T_{2g}$	$A_{1g}, T_{1g}, E_g, T_{2g}$	T_{1u}
$T(23)$	$A+E+2T$	A, E, T	T
$T_h(m3)$	$A_g+E_g+2T_g$	A_g, E_g, T_g	T_u
$O(434)$	$A_1+E+T_1+T_2$	A_1, E, T_1, T_2	T_1

Table 4
Linear molecules

Point group	$\Gamma(i^m\beta''^{cc}_{ijk})$	Active modes	
		beta	infrared
$C_{\infty v}$	$2\Sigma^+ + \Sigma^- + 2\Pi + \Delta$	$\Sigma^+, \Sigma^-, \Pi, \Delta$	Σ^+, Π
C_∞	$3\Sigma + 2\Pi + \Delta$	Σ, Π, Δ	Σ, Π
$D_{\infty h}$	$2\Sigma_g^+ + \Sigma_g^- + 2\Pi_g + \Delta_g$	$\Sigma_g^+, \Sigma_g^-, \Pi_g, \Delta_g$	Σ_u^+, Π_u^+
D_∞	$2\Sigma^+ + \Sigma^- + 2\Pi + \Delta$	$\Sigma^+, \Sigma^-, \Pi, \Delta$	Σ^-, Π

vibrational transition, using the rule (54) and the rules [6] governing products of irreducible representations of a given point group. In an allowed transition the product (54) must contain the TSR at least once. It is clear from table 3 that there are more beta active modes for the same molecule than infrared active modes (and there may be some beta active optical NMR modes that are neither infrared nor Raman active, in analogy with active modes in hyper-Raman scattering [33,34]).

It is well known [6] that standard point group character tables contain entries in their last columns which are combinations of Cartesian components representing infrared and Raman active modes. Each irreducible representation of a given molecular/crystallographic point group is associated with a given combination of scalar elements. Similarly, the irreducible representation can also be expressed in terms of combinations of Cartesian or spherical tensor components of the beta tensor, and details of how these combinations are derived are given in appendix A. Point group character tables for optical NMR can be constructed, in which each irreducible representation is matched with a combination of scalar elements of the relevant imaginary part of beta.

6. FMD computer simulation

This section reports a field applied molecular dynamics (FMD) computer simulation [27] of the effect of the beta tensor on an ensemble of 108 molecules of water. FMD computer simulation investigates classically the effect of an external torque on an ensemble of interacting molecules which are in general translating, rotating, and vibrating. It was initially developed [36,37] to describe the interaction of an external static electric field $\boldsymbol{E}^{(0)}$ with the permanent molecular electric dipole moment $\boldsymbol{\mu}$, through a torque on each molecule of type

$$\boldsymbol{T}_E = -\boldsymbol{\mu}\times\boldsymbol{E}^{(0)} . \tag{55}$$

Note that the integral over this torque with respect to configuration is the work done, which is minus the potential energy generated. The torque (55) therefore corresponds to a term

$$\Delta H_E = -\boldsymbol{\mu}\cdot\boldsymbol{E}^{(0)} \tag{56}$$

in the Hamiltonian. Such a term is the usual starting point of the semi-classical [13] or classical statistical mechanics [48] analysis of the molecular dynamics in for example dielectric and far infrared {48} spectroscopy, and it follows that FMD is as general a method of describing these dynamics, with the additional advantages to be described in this section and in the literature [27] of being able to give precise details of the time evolution of quantities such as correlation functions.

The torque relevant to the beta part of the optical NMR interaction energy is

$$\boldsymbol{T} = -(\boldsymbol{m}^{(\mathrm{ind})})_c \times \boldsymbol{B}^{(0)} , \tag{57}$$

where $(\boldsymbol{m}^{(\mathrm{ind})})_c$ is the classical magnetic dipole moment induced in each molecule by the conjugate product (1) of the circularly polarised laser. Note that the torque is generated through the cross product of $(\boldsymbol{m}^{(\mathrm{ind})})_c$ with the static magnetic flux density $\boldsymbol{B}^{(0)}$ of the permanent magnet of the NMR spectrometer. It occurs in addition to the well known torque

$$\boldsymbol{T}^{(\mathrm{NMR})} = -\boldsymbol{m}^{(\mathrm{N})} \times \boldsymbol{B}^{(0)} \tag{58}$$

set up [25] between $\boldsymbol{B}^{(0)}$ and the permanent magnetic dipole moment of the nucleus. The torque (58) is the basis for much of the textbook development of conventional NMR theory, for example the development leading to the Bloch equations [25]. It would be possible to carry out an FMD simulation of either type of torque, or both in combination, but we have limited the consideration to the torque

$$\begin{aligned} T_1 &= 2e_{2Z}e_{3Z}({}^{\mathrm{m}}\beta''^{\mathrm{cc}}_{312} - {}^{\mathrm{m}}\beta''^{\mathrm{cc}}_{231})_c E_0^2 B_Z^0 , \\ T_2 &= 2e_{1Z}e_{3Z}({}^{\mathrm{m}}\beta''^{\mathrm{cc}}_{123} - {}^{\mathrm{m}}\beta''^{\mathrm{cc}}_{312})_c E_0^2 B_Z^{(0)} , \\ T_3 &= 2e_{1Z}e_{2Z}({}^{\mathrm{m}}\beta''^{\mathrm{cc}}_{231} - {}^{\mathrm{m}}\beta''^{\mathrm{cc}}_{123})_c E_0^2 B_Z^{(0)} , \end{aligned} \tag{59}$$

generated in an ensemble of C_{2v} water molecules through eq. (57) written in the frame (1,2,3) of water. This torque is written in the same notation as eq. (16) for the $\boldsymbol{m}^{(\mathrm{ind})}$ components in frame (1,2,3) of the water molecule. The torque (59) is finally back transformed [40] into (X, Y, Z) coordinates using a convenient rotation matrix such as

$$\begin{pmatrix} T_X \\ T_Y \\ T_Z \end{pmatrix} = \begin{pmatrix} e_{1X} & e_{2X} & e_{3X} \\ e_{1Y} & e_{2Y} & e_{3Y} \\ e_{1Z} & e_{2Z} & e_{3Z} \end{pmatrix} \begin{pmatrix} T_1 \\ T_2 \\ T_3 \end{pmatrix} \tag{60}$$

and coded into the forces loop of a standard molecular dynamics algorithm, in this case TETRA [27]. (An entirely analogous procedure is possible for any standard MD code, for example GROMOS [49], designed for solvated protein segments, e.g. a Z-DNA segment in water.)

The water molecules interact through a site–site potential

$$\sigma_{ij}(r_i, r_j) = 4\epsilon\left[\left(\frac{\sigma}{r_{ij}}\right)^{12} - \left(\frac{\sigma}{r_{ij}}\right)^{6}\right] + \text{charge–charge}\,,$$

$$\sigma_{ij} = \sum\sum \phi_{ij}(\text{site–site})\,, \qquad (61)$$

$$\frac{\epsilon}{k}(\text{H–H}) = 21.1\ \text{K}\,, \quad \sigma(\text{H–H}) = 2.25\ \text{Å}\,,$$

$$\frac{\epsilon}{k}(\text{O–O}) = 58.4\ \text{K}\,, \quad \sigma(\text{O–O}) = 2.80\ \text{Å}\,,$$

$$q_{\text{H}} = 0.23|e|\,,$$

$$q(\text{lone pair}) = -0.23|e|\,,$$

$$q_0 = 0.00|e|\,,$$

developed [50] from the ST2, and compared [51] with the ab initio MCYL and with experimental water data [52] over a wide thermodynamic range. In the above representation ϵ/k and σ are atom–atom Lennard-Jones parameters, and q_{H} etc. represent partial charges from the ST2 model.

A sample of 108 water molecules was first equilibrated from an initial lattice into the liquid state at 293 K, 1.0 bar, with about 6000 time steps of 0.5 fs each. The torque (59) was then applied and second-order rise transients recorded of the type

$$\begin{array}{ccc} \langle e_{1X}^2\rangle & \langle e_{2X}^2\rangle & \langle e_{3X}^2\rangle \\ \langle e_{1Y}^2\rangle & \langle e_{2Y}^2\rangle & \langle e_{3Y}^2\rangle \\ \langle e_{1Z}^2\rangle & \langle e_{2Z}^2\rangle & \langle e_{3Z}^2\rangle \end{array}$$

for comparison (section 7) with generalised Langevin–Kielich functions. The rise transients gradually reach saturation, where they indicate that the torque (59) has brought the ensemble into "field-applied equilibrium", a statistically stationary state in which it is possible to analyse the sample with time correlation functions [48] computed by running time averaging over a minimum of 6000 time steps at field applied equilibrium. As most ACFs and CCFs are damped in a time window of less than 500 time steps, this gives good statistics.

As described in the literature [27,36–41] there is a well defined set of time correlation functions available to FMD which may not be accessible to standard diffusion theory [53]. The set includes auto- and cross-correlation functions (ACFs and CCFs), respectively diagonal and off-diagonal elements of the complete tensor product of the correlated variables. Attention in this section is restricted to ACFs and CCFs of orientation, rotational velocity and angular momentum, respectively defined by

$$C_{1ij}(t) = \frac{\langle e_{1i}(t)e_{1j}(0)\rangle}{\langle e_{1i}^2\rangle^{1/2}\langle e_{1j}^2\rangle^{1/2}}\,, \qquad (62)$$

by

$$C_{2ij}(t) = \frac{\langle \dot{e}_{1i}(t)\dot{e}_{1j}(0)\rangle}{\langle \dot{e}_{1i}^2\rangle^{1/2}\langle \dot{e}_{1j}^2\rangle^{1/2}} \qquad (63)$$

and by

$$C_{3ij}(t) = \frac{\langle J_i(t)J_i(0)\rangle}{\langle J_i^2\rangle^{1/2}\langle J_j^2\rangle^{1/2}}\,. \qquad (64)$$

Here $\boldsymbol{e}_1$ is the unit vector in the symmetry (i.e. permanent electric dipole) axis of the water molecule; $\dot{\boldsymbol{e}}_1$ is its time derivative; and $\boldsymbol{J}$ is the total net angular momentum of the water molecule. All three of these molecular dynamical quantities are defined as the sum of the natural (thermal) quantity plus that induced by the torque (59).

The effect of the beta tensor on the molecular dynamics of the water ensemble is represented through ACFs and CCFs of $\boldsymbol{e}_1$, $\dot{\boldsymbol{e}}_1$, and $\boldsymbol{J}$ components in figs. 3 to 8. These figures illustrate individual components of the ACFs and CCFs in the laboratory frame (X, Y, Z). For ACFs, the components are: $i=j=X$, and Z, respectively, referring to the subscripts of eqs. (62) to (64); for CCFs the plotted components are $i=X$, $j=Y$ and $i=Y$, $j=X$. These components are plotted for the angular momentum, orientation, and rotational velocity ACFs in figs. 3, 4 and 5, respectively, and for the corresponding CCFs in figs. 6, 7 and 8, respectively. Each figure is subdivided into two examples, corresponding respectively to: (a) elements ${}^{\text{m}}\beta''^{\text{ccc}}_{123}$, ${}^{\text{m}}\beta''^{\text{ccc}}_{231}$, and ${}^{\text{m}}\beta''^{\text{ccc}}_{312}$ in the ratio 1:2:3; (b) these same elements in the ratio 1:4:9. These arbitrary ra-

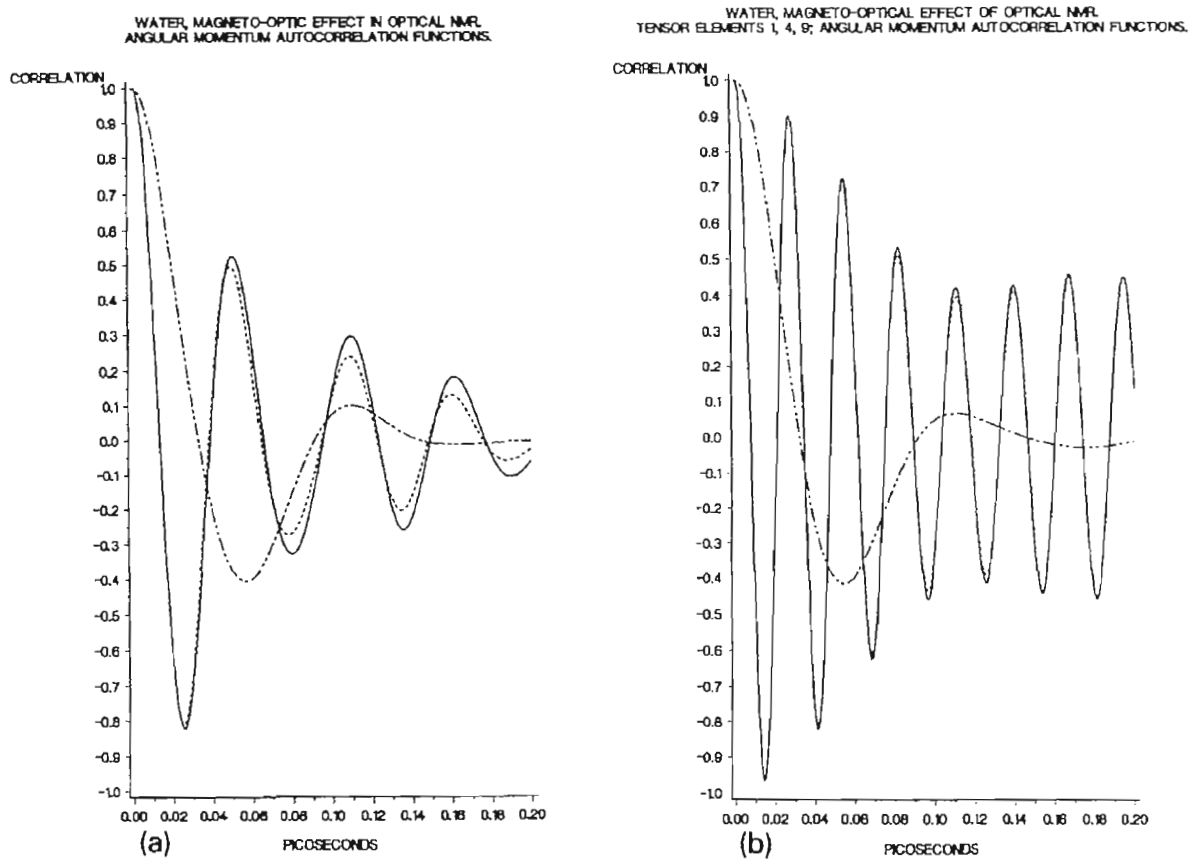

Fig. 3. Angular momentum ACFs from the computer simulation of optical NMR. - XX; — YY; -..-..- ZZ. (a) Tensor elements 1:2:3. (b) Tensor elements 1:4:9.

tios are used to illustrate the dependence of the correlation functions on details of the individual scalar elements of the optical NMR beta tensor, and are used in the absence of ab initio data on these elements. An ab initio computation of the elements of beta is most desirable, and can be carried out with a contemporary package such as HONDO [54] with the appropriate modifications. We shall not pursue this subject here.

It can be seen from figs. 3 to 5 that the effect of the torque (59) is to produce oscillations and anisotropy in the individual ACF elements, the $i=j=Z$ component evolves on a different scale, and this is the component corresponding to the Z-axis of propagation of the laser, parallel to the direction of $B_Z^{(0)}$ of the permanent magnet. The other two components oscillate with identical time dependencies within the noise. The oscillation frequency and amplitude patterns are markedly different for cases (a) and (b) for each ACF. The torque also makes possible the existence in the laboratory frame (X, Y, Z) of CCFs, which are illustrated in figs. 6 to 8. These CCFs are characteristic of optical NMR, and disappear in the absence of the torque. (The ACFs in the absence of the torque are isotropic, and are free of oscillations. They are illustrated in the literature [27].)

7. Rise transients and Langevin–Kielich functions of optical NMR

The second-order rise transients introduced in section 6 can be compared with analysis using generalised Langevin–Kielich functions. The derivation of the latter, in appropriate triple integral form, is given in Appendix B. The evaluation of the triple integral was accomplished numerically, using a program which incorporated IBM software [55] for double and single Gauss–Legendre quadrature, using a $48\times24\times24$ integration grid. The latter produced ac-

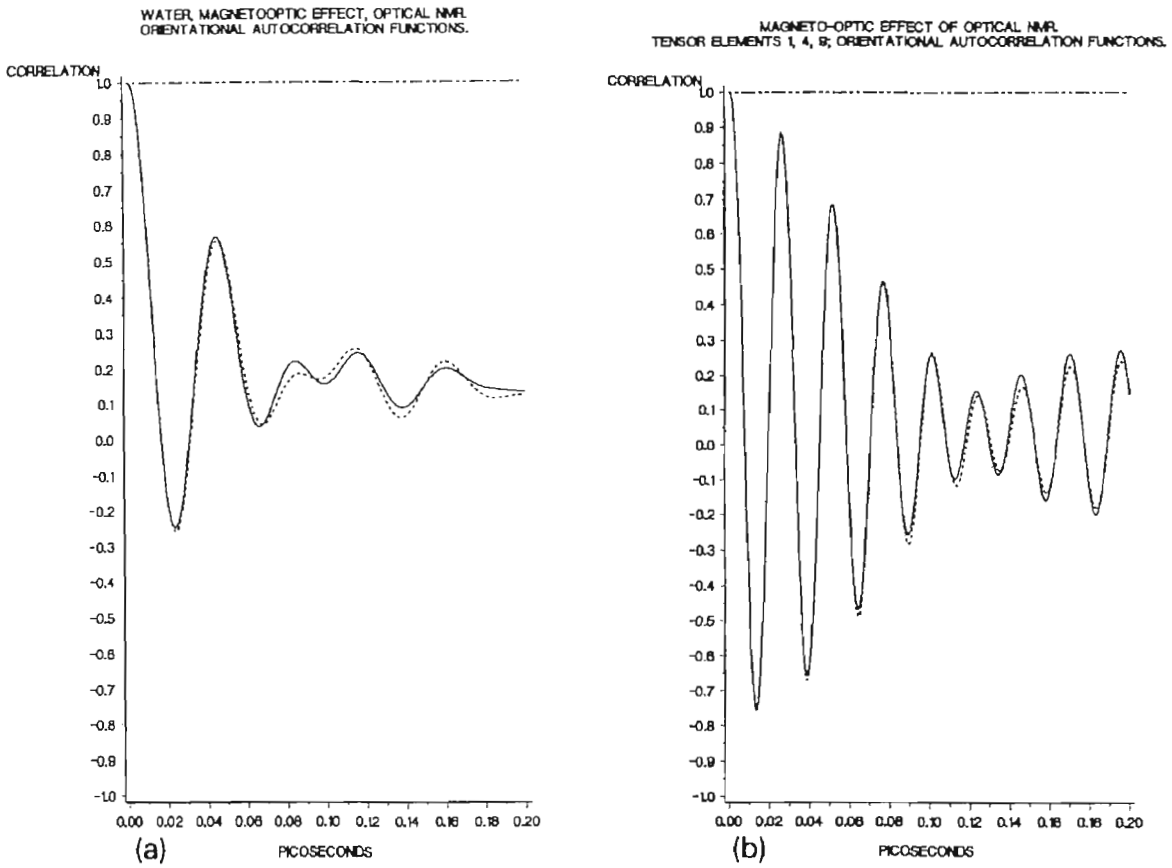

Fig. 4. As fig. 3; orientational ACFs from the computer simulation of optical NMR.

curacy to about six decimal places in the worst case and better than eleven decimal places in the best, estimates derived by numerical evaluation from the triple integral of first-order averages such as $\langle e_{1X} \rangle$, $\langle e_{2Y} \rangle$ and $\langle e_{3Z} \rangle$ which vanish through symmetry and in the computer simulation. Accuracy was checked also by changing the grid to $24 \times 24 \times 24$, with the result that no discernible changes were observable in the computed $\langle e_{1i}^2 \rangle$, $\langle e_{2i}^2 \rangle$ and $\langle e_{3i}^2 \rangle$ by the triple integral. Second-order rise transients from the latter reach a measurable saturation level, which is a point on the triple integral function for given $E_0^2 B_Z^{(0)}$. Comparison of simulated and computed generalised Langevin–Kielich functions then proceeded by comparison of the functions from the triple integral and from the simulation for several $E_0^2 B_Z^{(0)}$. The results are illustrated in fig. 9 for a beta component ratio of ${}^{m}\beta''^{ee}_{123} : {}^{m}\beta''^{ee}_{231} : {}^{m}\beta''^{ee}_{312}$ of 1:4:9.

For experimentally accessible $E_0^2 B_Z^{(0)}$ only the initial (linear) portion of the triple integral function needs to be used, as described in appendix B. The FMD simulation and triple integral results are in satisfactory agreement, however, throughout the range of development of the orientation functions, i.e. linear to saturation.

8. Discussion

The experimental development of optical NMR would provide information initially [26] on the shifting of conventional NMR lines with a low-intensity circularly polarised laser according to the guidelines given already. The shifting represents extra spectral structure of the type developed with Landé theory or dipole–dipole coupling in section 3. A shift of about 1.0 Hz is at the limit of the resolution [26] of the best contemporary apparatus, and theoretically needs an intensity of about 10 W/mm^2 delivered into the sample tube of an NMR spectrometer through a device such as an optical fibre. This type of investigation is currently in progress in the group of

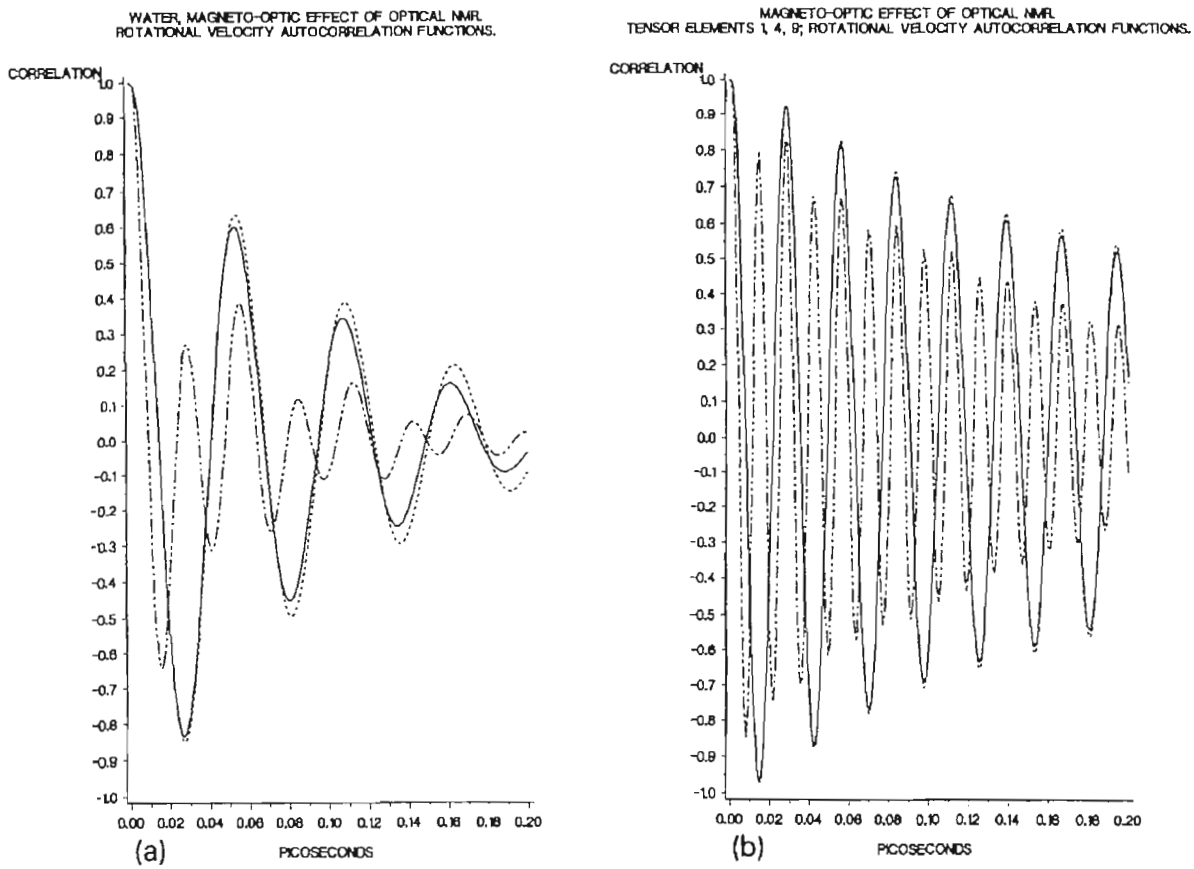

Fig. 5. As fig. 3; rotational velocity ACFs from the computer simulation.

Warren et al. [26]. An intensity of 10 W/mm^2 can be achieved using a 10 W circularly polarised laser (e.g. CW argon ion laser) passed through an optical fibre of area 1 mm^2. However, in structurally achiral chromophores, the optical fibre must conserve the circular polarisation qualities of the radiation delivered from the laser. Chiral chromophores may cause initially unpolarised radiation in the fibre to become elliptically polarised as it passes through the sample, but for maximum effect, the greatest degree of circular polarisation is needed in the radiation before it enters the sample held in the tube of an NMR spectrometer. Artifact elimination must concentrate on the efficient removal of heating effects, either by thermostatting or by using a flow chamber, or similar device. To separate artifacts from the beta and laser shift effects suggested in this paper, heating should be present independently of the polarisation characteristics of the laser, and the beta effects should vanish when the laser is not circularly polarised. Switching the laser from right to left circular polarisation should cause a discernible shift from one side of the original (conventional) NMR line to the other.

If the beta shifting is successfully isolated from artifacts it represents information on the coupling between the laser induced electronic angular momentum and the nuclear net angular momentum. It follows that the shift depends on electronic as well as nuclear properties of the chromophore, and therefore has some characteristics of ESR and NMR "in combination". Beta and dipole–dipole shifting should therefore be different for each nuclear resonating site (for example a proton in a different electronic environment). This site selectivity should be of particular interest in the investigation fo samples with many different proton sites, such as folded proteins in solution. Each original proton resonance line of the conventional NMR spectrum should be shifted to a different extent, so that a 2-D NMR contour map is changed "geographically" as mentioned already.

It appears not unduly optimistic to expect that site selective shifting of NMR resonances will be useful

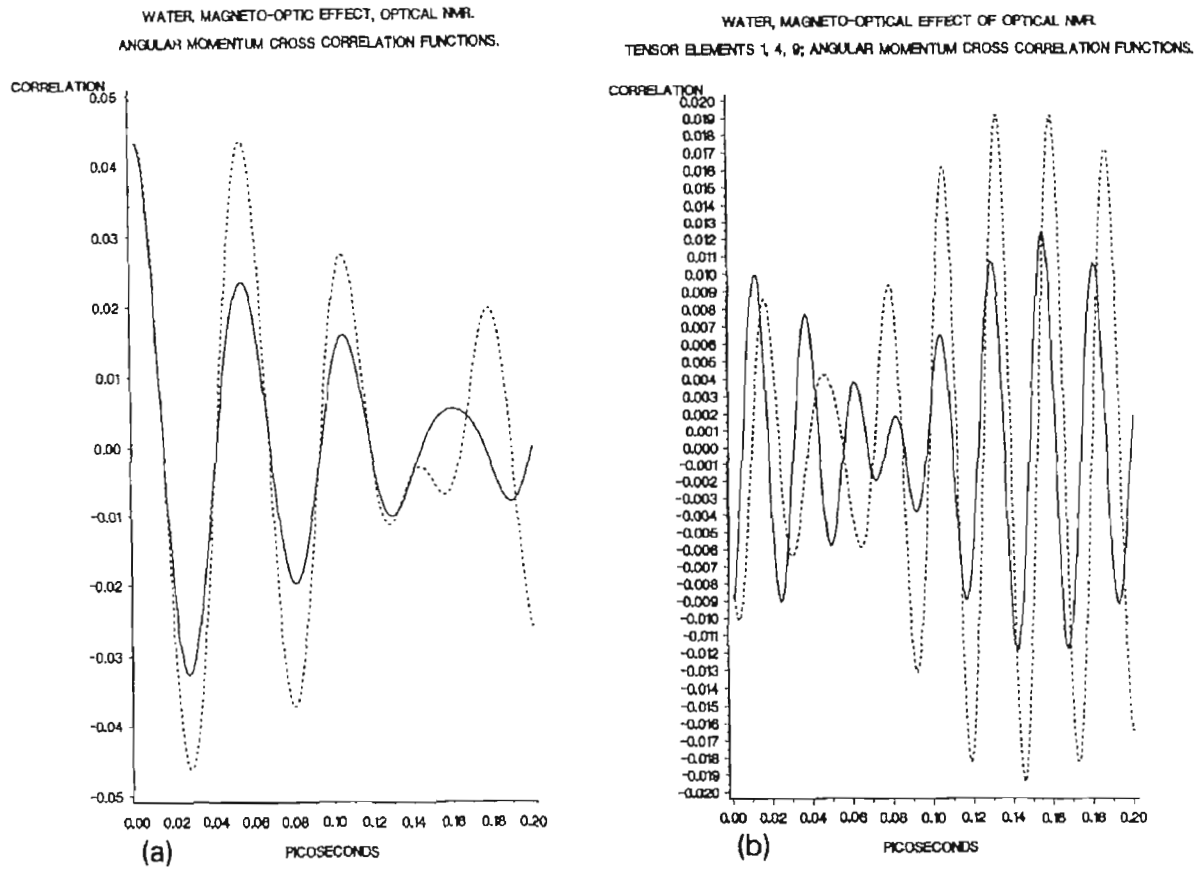

Fig. 6. Angular momentum CCFs from the computer simulation: —XY; —YX components. (a) and (b) as figs. 3 to 5.

even if the underlying quantum structure is not resolved. The shift should be sensitive to tuning to resonance, as described in section 4, and in this context different pump lasers operating at different frequencies throughout the ultraviolet, visible and infrared range are available. Tuning to resonance should increase the shift for constant laser intensity I. Alternatively, by tuning in this way, a much lower I would be needed than at a transparent frequency. However, tuning to resonance must be carried out with an efficient thermostat, in order to remove heating by absorption. Again this artifact can be recognised by the fact that it would occur with a laser that is unpolarised, while beta shifting cannot occur with an unpolarised laser.

Optical NMR according to section 3 of this paper offers the potential of revealing detailed structure due to Landé and dipole–dipole coupling, and increased absolute frequency separation of resonance features, both useful developments in analysis. Resolution of the quantum structure requires the use of more intense lasers and pulsing techniques. In theory, I can be increased by mode locking or Q-switching by many orders of magnitude, causing an equivalent shift in the original NMR line. If the technology can be developed to produce this effect, the consequences are surely of widespread interest, since the beta theory presented in this paper combines two major contemporary fields of research, NMR and laser spectroscopy.

Acknowledgement

MWE thanks the Swiss NSF (Bern) for the award of a Senior Fellowship and the University of Zurich for a Visiting Scientist position. ETH is thanked by MWE for a major grant of computer time on the IBM 3090 supercomputer, with which the numerical work for this paper was carried out. Prof. G. Wagnière and Prof. S. Woźniak are thanked for many interesting discussions, particularly concerning the material in

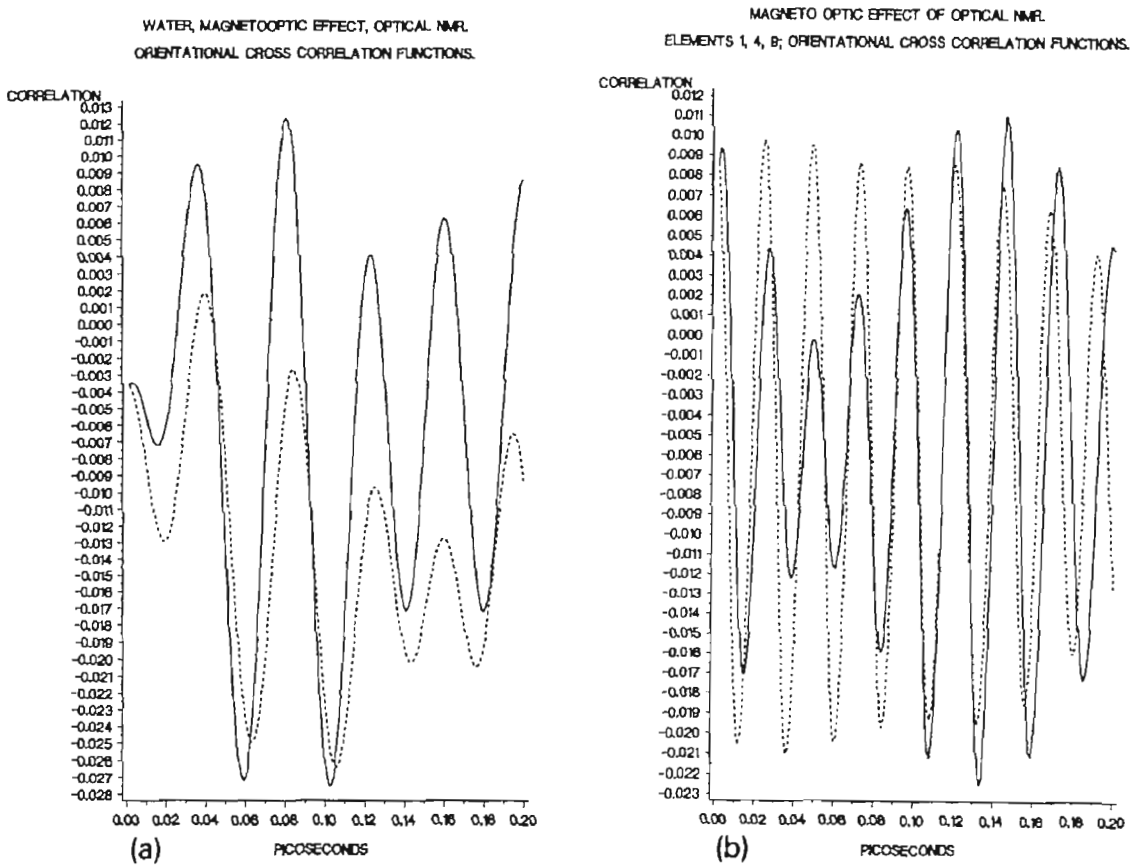

Fig. 7. As fig. 6; orientation CCFs from the computer simulation.

the appendices. Dr. Laura J. Evans is thanked for invaluable help with the SAS plotting facility of the Irchel mainframe computer of the University of Zurich. Prof. Warren Sloan Warren of the Department of Chemistry at Princeton University is thanked for many discussions and e-mail correspondence concerning the prototype experiment.

Appendix A. Irreducible Cartesian components of the beta tensor

The third rank tensor ${}^{\mathrm{m}}\beta''^{\mathrm{ee}}_{ijk}$ can be reduced to irreducible Cartesian components of weights zero, one and two. The weight-zero component is

$$\beta^{(0)} = \epsilon_{ijk}\, {}^{\mathrm{m}}\beta''^{\mathrm{ee}}_{ijk} \tag{A.1}$$

and for molecules of C_{2v} symmetry such as water

$$\beta^{(0)} = 2({}^{\mathrm{m}}\beta''^{\mathrm{ee}}_{123} + {}^{\mathrm{m}}\beta''^{\mathrm{ee}}_{231} + {}^{\mathrm{m}}\beta''^{\mathrm{ee}}_{312}) . \tag{A.2}$$

In tables 1 and 2 the weight-zero parts can be found for other molecular point groups, and incorporated in point group character tables.

Similarly, the weight-one component is

$$\beta^{(1)} = \tfrac{1}{2}(\delta_{ij}(\beta_1^{\{1\}})_k + \delta_{ik}(\beta_2^{\{1\}})_j) , \tag{A.3}$$

with

$$(\beta_1^{\{1\}})_j \equiv {}^{\mathrm{m}}\beta''^{\mathrm{ee}}_{iij} = {}^{\mathrm{m}}\beta''^{\mathrm{ee}}_{11j} + {}^{\mathrm{m}}\beta''^{\mathrm{ee}}_{22j} + {}^{\mathrm{m}}\beta''^{\mathrm{ee}}_{33j} ,$$

$$(\beta_2^{\{1\}})_j \equiv {}^{\mathrm{m}}\beta''^{\mathrm{ee}}_{iji} = {}^{\mathrm{m}}\beta''^{\mathrm{ee}}_{1j1} + {}^{\mathrm{m}}\beta''^{\mathrm{ee}}_{2j2} + {}^{\mathrm{m}}\beta''^{\mathrm{ee}}_{3j3} .$$

Finally, the weight-two component is

$$(\beta^{(2)})_{mnl} = \tfrac{1}{3}\epsilon_{mnk}[2(\beta_1^{\{2\}})_{kl} + (\beta_2^{\{2\}})_{kl}] + \tfrac{1}{3}[(\beta_1^{\{2\}})_{lk} + 2(\beta_2^{\{2\}})_{lk}]\epsilon_{kmn} , \tag{A.4}$$

with

$$(\beta_1^{\{2\}})_{kl} = -\tfrac{1}{2}(\epsilon_{kij}\, {}^{\mathrm{m}}\beta''^{\mathrm{ee}}_{jil} + \epsilon_{lij}\, {}^{\mathrm{m}}\beta''^{\mathrm{ee}}_{jik}) - \tfrac{1}{3}\beta^{(0)}\delta_{kl} ,$$

$$(\beta_2^{\{2\}})_{kl} = -\tfrac{1}{2}({}^{\mathrm{m}}\beta''^{\mathrm{ee}}_{lij}\epsilon_{jik} + {}^{\mathrm{m}}\beta''^{\mathrm{ee}}_{kij}\epsilon_{jil}) - \tfrac{1}{3}\beta^{(0)}\delta_{kl} .$$

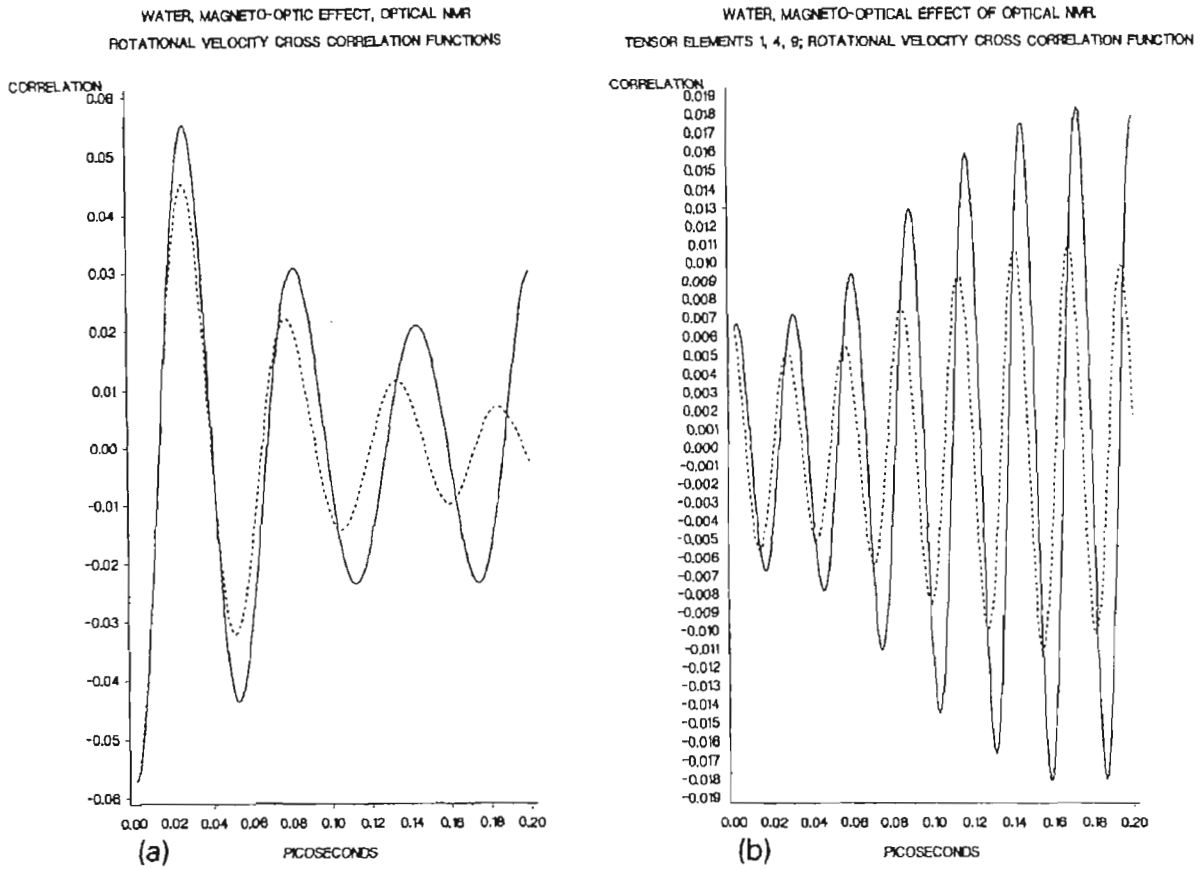

Fig. 8. As fig. 6; rotational velocity CCFs.

Appendix B. Langevin–Kielich triple integral

We are interested in the thermodynamic averages of unit vectors with the energy (10) of the text. This average must be worked out in the molecule fixed frame (see tables 1 and 2) where we know the symmetry of the beta tensor of optical NMR. This involves a transformation of the beta tensor from the laboratory frame (X, Y, Z) to the molecule fixed frame (1, 2, 3). Defining i, j, k subscripts as referring to the laboratory frame, and α, β, γ subscripts as referring to frame (1, 2, 3), the transformation of beta from one frame to the other is given in terms of unit vectors $\boldsymbol{e}_{i\alpha}$, $\boldsymbol{e}_{j\beta}$ and $\boldsymbol{e}_{k\gamma}$, which are directional cosines [13]

$$({}^{\mathrm{m}}\beta''^{\mathrm{ee}}_{ijk})(0;\omega,-\omega) = \boldsymbol{e}_{i\alpha}\boldsymbol{e}_{j\beta}\boldsymbol{e}_{k\gamma}({}^{\mathrm{m}}\beta''^{\mathrm{ee}}_{\alpha\beta\gamma})(0;\omega,-\omega)\,. \tag{B.1}$$

It follows that the thermodynamic average involves the three Euler angles. Expressing the unit vectors in terms of the Euler angles θ, ϕ, and χ gives the triple integral Langevin–Kielich function of the text. In the particular case of water the triple integral function expresses thermodynamic averages over Φ, where

$$\Phi = \cos^n\theta = e^n_{1Z}\,, \quad \text{or } \sin^n\phi\sin^n\phi = e^n_{2Z}\,, \quad \text{or } \sin^n\theta\cos^n\phi = e^n_{3Z} \tag{B.2}$$

are unit vector components in the direction of the Z-axis of the laboratory frame. In terms of the quantities

$$a = \frac{({}^{\mathrm{m}}\beta''^{\mathrm{ee}}_{231})}{({}^{\mathrm{m}}\beta''^{\mathrm{ee}}_{123})}\,, \quad b = \frac{({}^{\mathrm{m}}\beta''^{\mathrm{ee}}_{312})}{({}^{\mathrm{m}}\beta''^{\mathrm{ee}}_{123})}\,, \quad d = \frac{2\,{}^{\mathrm{m}}\beta''^{\mathrm{ee}}_{123}E_0^2B_0}{kT}\,, \tag{B.3}$$

the triple integral expression is

$$\langle\phi\rangle = \frac{\int_0^{2\pi}\int_0^{2\pi}\int_0^{\pi}\Phi\exp[f(\theta,\phi,\chi)]\,\mathrm{d}\theta\,\mathrm{d}\phi\,\mathrm{d}\chi}{\int_0^{2\pi}\int_0^{2\pi}\int_0^{\pi}\exp[f(\theta,\phi,\chi)]\,\mathrm{d}\theta\,\mathrm{d}\phi\,\mathrm{d}\chi}\,, \tag{B.4}$$

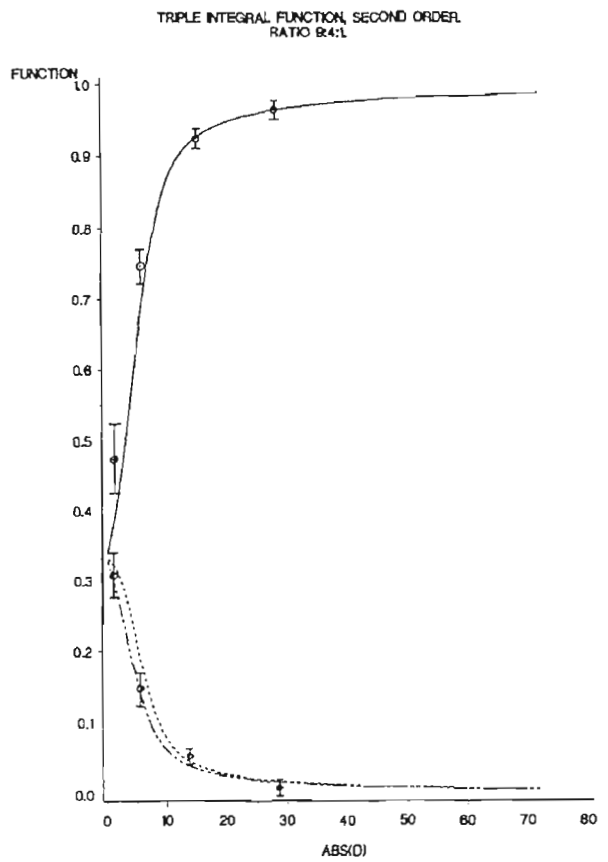

Fig. 9. Langevin–Kielich (triple integral) functions for $\langle e_{1Z}^2 \rangle$, $\langle e_{2Z}^2 \rangle$, $\langle e_{3Z}^2 \rangle$, matched with $\overline{\underline{\circ}}$ from final level of rise transients from simulation. —$\langle e_{1Z}^2 \rangle$; ----$\langle e_{2Z}^2 \rangle$; ·····$\langle e_{3Z}^2 \rangle$

$$f(\theta,\phi,\chi) = d(\cos^2\theta(\cos^2\phi\cos^2\chi + \sin^2\phi\sin^2\chi) + (a\sin^2\phi\cos^2\chi + b\cos^2\phi\sin^2\chi)\sin^2\theta + \tfrac{1}{4}((a+b+1)\sin^2\theta - 2) \times \cos\theta\sin 2\phi\sin 2\chi)\sin\theta\,. \qquad (B.5)$$

References

[1] P.S. Pershan, Phys. Rev. 130 (1963) 919.
[2] J.P. van der Ziel, P.S. Pershan and L.D. Malmstrom, Phys. Rev. Letters 15 (1965) 190.
[3] P.S. Pershan, J.P. van der Ziel and L.D. Malmstrom, Phys. Rev. A 143 (1966) 574.
[4] L.D. Barron, Chem. Soc. Rev. 15 (1986) 189.
[5] P.W. Atkins and M.H. Miller, Mol. Phys. 15 (1968) 503.
[6] P.W. Atkins, Molecular Quantum Mechanics, 2nd ed. (Oxford Univ. Press, Oxford, 1983).
[7] Y.R. Shen, The Principles of Non-Linear Optics (Wiley, New York, 1984).
[8] S. Woźniak, B. Linder and R. Zawodny, J. Phys. (Paris) 44 (1983) 403;
S. Kielich, N.L. Manakov and V.D. Ovsiannikov, Acta Phys. Polon. A 53 (1978) 595, 581, 737.
[9] S. Woźniak and R. Zawodny, Phys. Letters A 85 (1981) 111.
[10] S. Woźniak, Mol. Phys. 59 (1986) 421.
[11] S. Woźniak, G. Wagnière and R. Zawodny, Phys. Letters A 154 (1991) 259.
[12] G. Wagnière, Phys. Rev. A 40 (1989) 2437.
[13] L.D. Barron, Molecular Light Scattering and Optical Activity (Cambridge Univ. Press, Cambridge, 1982).
[14] M.W. Evans, Phys. Rev. Letters 64 (1990) 2909.
[15] M.W. Evans, Opt. Letters 15 (1990) 863.
[16] M.W. Evans, J. Mol. Spectry 146 (1991) 143.
[17] M.W. Evans, Physica B 168 (1991) 9.
[18] M.W. Evans, J. Phys. Chem. 95 (1991) 2256.
[19] M.W. Evans and C.R. Pelkie, J. Opt. Soc. Am. B, in press, 1991, with video animation.
[20] S. Woźniak and R. Zawodny, Acta Phys. Polon. A 61 (1982) 175.
[21] G. Wagnière and A. Meier, Chem. Phys. Letters 93 (1982) 78.
[22] G. Wagnière, Z. Naturforsch. 39 a (1984) 254.
[23] L.D. Barron and J. Vrbancich, Mol. Phys. 51 (1984) 715.
[24] L.D. Barron, in: New Developments in Molecular Chirality, ed. P.G. Mezey (Reidel, Amsterdam, 1990).
[25] C.P. Slichter, Principles of Magnetic Resonance, 2nd ed. (Springer, Berlin, 1978).
[26] W.S. Warren et al., Dept. of Chemistry, Princeton University, discussions and e-mail communications, August 1990, to present.
[27] M.W. Evans, in: eds. I. Prigogine and S.A. Rice, Advances in Chemical Physics, Vol. 81 (Wiley Interscience, New York, 1991) in press, with ca. 450 refs.
[28] G. Wagner, Prog. NMR Spectrosc. 22 (1990) 101.
[29] K. Gorell, V. Sik and W. Stephenson, Prog. NMR Spectrosc. 22 (1990) 141.
[30] S.W. Howan, Prog. NMR Spectrosc. 22 (1990) 55.
[31] G. Wagnière and J.B. Hutter, J. Opt. Soc. Am. B 6 (1989) 695.
[32] M. Weissbluth, Photon Atom Interactions (Academic Press, London, 1989).
[33] T. Bancewicz, Z. Ozgo and S. Kielich, J. Raman Spectrosc. 1 (1973) 177.
[34] L. Stanton, J. Raman Spectrosc. 1 (1973) 53.
[35] S. Kielich, in: Dielectric and Related Molecular Processes, Vol. 1 (Chem. Soc., London, 1972).
[36] M.W. Evans, J. Chem. Phys. 76 (1982) 5473, 5480.
[37] M.W. Evans, J. Chem. Phys. 77 (1982) 4632; 78 (1983) 925; 79 (1983) 5403.
[38] M.W. Evans, G.C. Lie and E. Clementi, J. Chem. Phys. 87 (1987) 6040.
[39] M.W. Evans, G.C. Lie and E. Clementi, Phys. Letters A 130 (1988) 289.
[40] M.W. Evans and G. Wagnière, Phys. Rev. A 42 (1990) 6732.

[41] S. Woźniak, G. Wagnière and M.W. Evans, Mol. Phys., in press, parts 1 and 2.
[42] M.W. Evans, Phys. Rev. A 39 (1989) 6041; 40 (1990) 4601.
[43] M.W. Evans, Chem. Phys. 135 (1989) 187; 132 (1989) 1.
[44] R. Zare, Angular Momentum (Wiley, New York, 1988).
[45] C.H. Townes and A.L. Schawlow, Microwave Spectroscopy (McGraw-Hill, New York, 1955; Dover, New York, 1975) Ch. 11.
[46] M.W. Evans, Mol. Phys. 71 (1990) 193.
[47] E.B. Wilson Jr., J.C. Decius and P.C. Cross, Molecular Vibrations (McGraw-Hill, New York, 1955).
[48] M.W. Evans, G.J. Evans, W.T. Coffey and P. Grigolini, Molecular Dynamics (Wiley Interscience, New York, 1982).
[49] GROMOS Manual and Code, communicated by Prof. Dr. W.F. van Gunsteren, ETH, Zurich, April, 1991.
[50] M.W. Evans, J. Mol. Liq. 34 (1987) 269.
[51] M.W. Evans, K.N. Swamy, K. Refson, G.C. Lie and E. Clementi, Phys. Rev. A 36 (1988) 3935.
[52] M.W. Evans, G.C. Lie and E. Clementi, J. Chem. Phys. 88 (1988) 5157.
[53] M.W. Evans, P. Grigolini, G. Pastori, I. Prigogine and S.A. Rice, eds., Advances in Chemical Physics, Vol. 62, 63 (Wiley Interscience, New York, 1985).
[54] E. Clementi, ed., MOTECC 90 (Escom, Leiden, 1990).
[55] IBM ESSL Library, Routines DFLNQ and DFLNQ2, ETH Zurich, IBM 3090 implementation.